

ELECTRICAL AND RADIATION CHARACTERISTICS OF WATER IN THE
DECIMETER AND METER RANGE

V. Yu. Rayzer, Ye. A. Sharkov, and V. S. Etkin

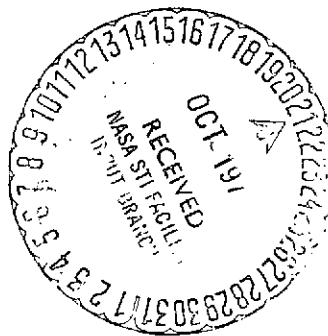
(NASA-TT-F-15967) ELECTRICAL AND
RADIATION CHARACTERISTICS OF WATER IN THE
DECIMETER AND METER RANGE (Kanner (Leo)
Associates) 68 p HC \$6.50 CSCL 07D

N74-33884

Unclas

G3/13 50394

Translation of ^aElektricheskiye i izluchatel'nyye kharacter-
istiki vody v detsimetrovom i metrovom diapazonakh, Institute
of Space Research, USSR Academy of Sciences, Report Pr-164,
Moscow, 1974, pp. 1-46, plus figures



STANDARD TITLE PAGE

1. Report No. NASA TT F-15,967	2. Government Accession No.	3. Recipient's Catalog No.	
4. Title and Subtitle ELECTRICAL AND RADIATION CHARACTERISTICS OF WATER IN THE DECIMETER AND METER RANGE		5. Report Date October 1974	6. Performing Organization Code
7. Author(s) V. Yu. Rayzer, Ye. A. Sharkov, and V. S. Etkin		8. Performing Organization Report No.	10. Work Unit No.
9. Performing Organization Name and Address Leo Kanner Associates Redwood City, California 94063		11. Contract or Grant No. NASw-2481	13. Type of Report and Period Covered
12. Sponsoring Agency Name and Address National Aeronautics and Space Admini- stration, Washington, D.C. 20546		14. Sponsoring Agency Code	
15. Supplementary Notes Translation of Elektricheskiye i izluchatel'nyye kharakter- istiki vody v detsimetrovom i metrovom diapazonakh, Institute of Space Research, USSR Academy of Sciences, Report Pr-164, Moscow, 1974, pp. 1-46 plus figures			
16. Abstract An examination is made of the effect of the temperature and salinity of sea water on its dielectric constants and the radiation characteristics of a smooth water surface in the 10-200 cm wavelength range. With reference to the dependence of the dielectric constants on temperature and salinity, and also the effect of atmospheric glow, it was shown that the optimal working range of the working wavelengths for investigating the distribution of the salinity of the ocean by passive remote methods is the 60-80 cm range. And a 43.5° K decrease in the radiobrightness temperature corres- ponds to a 0-30 per mil salinity change, at the wavelength of 75 cm and the radiating surface temperature of 20°C. Experimental material is compared with the theoretical cal- culations.			
17. Key Words (Selected by Author(s))		18. Distribution Statement Unlimited - Unclassified	
19. Security Classif. (of this report) Unclassified	20. Security Classif. (of this page) Unclassified	21. No. of Pages 68	22. Price

AUTHORS' ABSTRACT

/2

An examination is made of the effect of the temperature and salinity of sea water on its dielectric constants and the radiation characteristics of a smooth water surface in the 10-200 cm wavelength range. With reference to the dependence of the dielectric constants on temperature and salinity, and also the effect of atmospheric glow, it was shown that the optimal working range of the working wavelengths for investigating the distribution of the salinity of the ocean by passive remote methods is the 60-80 cm range. And a 43.5° K decrease in the radiobrightness temperature corresponds to a salinity change of 0 to 30 per mil, at the wavelength of 75 cm and radiating surface temperature of 20° C.

The experimental material was compared with the theoretical calculations.

INTRODUCTION

/3

Literature Review

To solve several scientific and applied problems (for example, remote probing of the Earth, and satellite meteorology and oceanology), detailed data on the electrical, radiation, and reflection characteristics of fresh and sea water are required over a wide range of wavelengths: from the millimeter to the meter and dekameter [sic] ranges.

Interpretation of the measurement of reflection and radiation characteristics of the water surface is possible only when data are available concerning the dielectric constants of solutions at different temperatures and salt concentrations.

The present study gives a detailed calculation of the dielectric characteristics of fresh and salt (NaCl solution)¹ water in the 0-40° C temperature range and the 0-40 per mil salinity range, based on the Debye polarization model [1, 2] for wavelengths from 10 to 200 cm. Calculation results are compared with available experimental data in this frequency range aimed at finding the applicability of the Debye polarization model for fresh and especially sea water, which is a subject of broad discussion [3, 2, 4, 5]. From the data in [5] it follows that the theoretical calculation of the characteristics in this case must be done with a relative precision not poorer than 0.1 percent.

¹ The problem of the effect of other salts is treated in Section 2.

Based on data on the dielectric characteristics, in the present study are presented calculations of the radiation and reflection characteristics of a quiet water surface² in the above-indicated temperature, frequency, and salinity ranges. In addition, the effect on the radiobrightness temperature of a quiet water surface exerted by temperature and salinity is discussed. Study of these dependences is important both from the standpoint of finding the possibilities of the remote investigation of the distribution of salinity and temperature, and from the methodological viewpoint, since calibrating radiometric onboard systems with respect to a quiet water surface is one of the most precise methods [7].

If the expression for the radiobrightness temperature must have a precision of the order of 0.2° K, the relative error in the calculations of emissivity must be better than 0.2 percent [8].

From the requirements of the problems formulated, all numerical results are represented in tabular form (the relative precision is about 0.1 percent), as well as in graphs.

We note that the domestic and foreign literature contains fragmentary reports on the dielectric constants and the radiation characteristics of sea water for certain mean values of temperature and salinity, and there are no data on the variation within the temperature and salinity ranges intrinsic to sea water in different parts of the World Ocean.

Available experimental data on the electrical characteristics of water are generalized in a number of recent reviews [9, 10, 4, 11].

² The problem of the radiation characteristics of a wave-agitated sea is the subject of special investigation (for example, [6]).

From studies on the theoretical calculation of the radiation characteristics of fresh and sea water, [7, 12] must be singled out. The first of these gives a detailed theoretical calculation of the effect of temperature and salinity on the radiation of a smooth water surface in the centimeter range (0.3-8.5 cm) by relying on the Debye relaxation model of polarization [7].

The emissivity of water in the range from the millimeter [5] to the meter waves is calculated in the second study [12]. However, in the calculations several assumptions are made; these lead to the apparent independence of the dielectric constant from salinity, which -- in turn -- strongly affects the magnitude of the emissivity of the ocean surface (see below).

In a recent study [13] based on the Debye model, the authors constructed functions similar to those examined below, however the precision of the plotting of the graphs (computer-aided) is poorer than 2 percent (in the estimates of the authors themselves). Also, there is no comparison with available experimental material and no allowance for atmospheric glow as affecting the radiobrightness temperature of the water surface.

A comparison of the calculation results given in the report with available experimental data is made in the appropriate sections.

ELECTRICAL AND RADIATION CHARACTERISTICS OF WATER IN THE DECIMETER AND METER RANGES

V. Yu. Rayzer, Ye. A. Sharkov, and V. S. Etkin

1. Electrical Characteristics of Fresh and Salt Water

The Debye dispersion model [1,2] is assumed in the calculation of the electrical characteristics of a smooth water surface. In the UHF range the real and the imaginary parts of the dielectric permittivity [dielectric constant] of water can be represented as [1,2]

$$\epsilon' = \frac{\epsilon_s - \epsilon_\infty}{1 + (\lambda_s/\lambda)^2} + \epsilon_\infty \quad (1)$$

$$\epsilon'' = \frac{\epsilon_s - \epsilon_\infty}{1 + (\lambda_s/\lambda)^2} \cdot \frac{\lambda_s}{\lambda} + 60 \epsilon \lambda \quad (2)$$

where λ_s is the critical wavelength, determined by the relaxation time of the water molecules

ϵ_s is the static dielectric constant,

ϵ_∞ is the optical dielectric constant,

λ is the radiation wavelength, and

σ is the specific electroconductivity of the NaCl solution. [6]

The dependence of the static dielectric constant on temperature is of the form [3]:

$$\epsilon_s = 87.74 - 0.4008t + 9.398 \cdot 10^{-4}t^2 - 1.410 \cdot 10^{-6}t^3 \quad (3)$$

with an error of 0.01 unit, where t is the water temperature in $^{\circ}\text{C}$.

The optical dielectric constant is assumed to be identical for salt and fresh water; the dependence of ϵ_∞ on temperature, according to [3], can be written in the form:

$$\epsilon_\infty = 5 + 0.02t \quad (4)$$

For aqueous solutions of sodium chloride, the values of λ_s and σ as functions of salinity³ and temperature were found by means of data in the reports [3,7]. Calculations of the dielectric constants of fresh and sea water for different temperatures and salinities were made on the basis of Eqs. (1) - (4), computer-aided. The results are presented in Tables 1 and 2 and in graphs.

The real part of the complex dielectric permittivity of both fresh and salt water increases with increase in the radiation wavelength in the range 0.3-10 cm, and for fresh water this rise with increase in water temperature proves to be more strongly pronounced.

When the wavelength is increased from 10 to 200 cm, ϵ' is virtually independent of λ . Its value for fresh water is somewhat higher than for salt; with increase in temperature, ϵ' falls off at the same salinity (Fig. 1).

³ The concepts of salinity and molar concentration are used in estimating the salt concentrations in solutions. By salinity (S) is understood the total amount of dry residue in grams isolated from one kilogram of sea water. Salinity is expressed in g/kg or in weight percent, that is, 1 weight percent = 10 g/kg = 10 per mil. (per mill.) [14]. In [5] the following formula is proposed, relating S per mil with the molar concentration (M) of NaCl in sea water: S per mil = 75.13 M (NaCl). As reference information we note that the mean salinity of the World Ocean is 35 per mil. For the Atlantic and Pacific oceans, 37.5 and 35 per mil, respectively, and 2-7 per mil for the Baltic Sea [14,8]. The validity of the model experiments in which sea water was replaced with an NaCl solution (as, for example, in [7]) must be carefully discussed in each case (see Section 2).

47

In the millimeter range (0.3-1 cm) generally there is no effect of salinity on ϵ' . In the decimeter and meter ranges the virtually identical variation of ϵ' with salinity change 0 to 40 per mil is observed, namely, about 15 percent of the relative change from the mean value of ϵ' ($t = 0^\circ \text{C}$).

From Fig. 1 it follows that the effect of temperature on ϵ' in the decimeter and meter ranges is of the same order as the effect of salinity, namely, with a temperature rise from 0 to 30°C the relative change in ϵ' is 14-16 percent.

We note that the effect of temperature on ϵ' in the millimeter and decimeter wavelength ranges varies: in the first region ϵ' rises with increase in temperature, while in the second -- it decreases.

The loss tangent for $\lambda = 0.3-1 \text{ cm}$ have a maximum for both fresh and salt water; it shifts toward the smaller wavelength side with increase in temperature (Fig. 2).

In the region $\lambda = 1-20 \text{ cm}$, $\text{tg } \delta$ for salt water has a minimum, shifted toward the side of longer wavelengths (all the way to 20 cm) with decrease in temperature (salinity kept constant), as well as with decrease in salinity (temperature kept constant).

For fresh water, even from $\lambda > 1 \text{ cm}$ the change in $\text{tg } \delta$ shows a linear decrease with respect to wavelength.

Like the dependence of the real part of the complex dielectric permittivity, $\text{tg } \delta$ is virtually independent of salinity in the millimeter range. In the decimeter and meter ranges, the conductivity of salt water causes a sharp rise in the loss tangent, which differs from its value for fresh water by two to three orders of magnitude (while ϵ' varies by about 15 percent in relative magnitude), which -- in turn -- is reflected in the radiation characteristics of salt water.

48

We note that in the range $\lambda = 5-20$ cm there is a change in the temperature dependence of the loss tangent for salt water, while for fresh water throughout nearly the entire wavelength range $\operatorname{tg} \delta$ decreases with increase in temperature.

To examine the further trend of the dependence of the loss tangent on wavelength for fresh water, we must know its conductivity, which has strong variations as a function of the type of fresh water. The specific conductivity of natural bodies of water varies within wide limits (from 10^2 to 10^{-3} (ohm-meter) $^{-1}$, (determined by the chemical composition of the water. And the maximum specific conductivities of the order of hundreds (ohm-meter) $^{-1}$ pertain to highly mineralized waters of petroleum deposits and certain ore waters.

The specific conductivities of the order of $0.125 \cdot 10^{-1} - 10^{-3}$ (ohm-m) $^{-1}$ are characteristic of ground and rain fresh water [157].

Values of specific conductivity of the order of $5 \cdot 10^{-6}$ (ohm-m) $^{-1}$ [157] are given for pure distilled water, which does not lead to a substantial change in $\operatorname{tg} \delta$ in this wavelength range.

Actually, the correction to the loss tangent for pure distilled water, with allowance for its specific conductivity in the meter wavelength range ($\lambda = 200$ cm) is of the order of 10^{-5} units. This correction decreases with decrease in wavelength, as can easily be seen from Eqs. (1) - (2). /9

Let us estimate the loss tangent for various natural waters in the meter wavelength ($\lambda = 200$ cm); it is 1000 - 1600, respectively, for the waters of petroleum deposits and certain ore waters and 2-0.1 for surface ground and rain water.

Hence it is clear that the loss tangents of various natural waters very strongly depends on the chemical composition of fresh water.

In the present study, it was assumed that the specific conductivity of fresh water is absent, i.e., $\sigma = 0$.

The report [12] contains analogous results of the calculation of the dielectric characteristics of sea and fresh water. However, in this study the effect of salt concentration is reduced only to changing the electroconductivity of the solution. This view leads to the independence of the real part of the complex dielectric permittivity on salinity. It is also assumed that the values of λ_s and ϵ_s are functions solely of temperature, which differs from those adopted here. It should be noted that the dependence of λ_s and ϵ_s on temperature in [12] was taken from earlier publications (1948). In contrast, the functions used in the present study are taken from 1961 publications. Also, in [12] the value of the optical constant ϵ_0 is identical for all temperatures, in contrast to Eq. (4). All this accounts for the discrepancies in the values of ϵ' and $\text{tg } \delta$, though the nature of their variation with respect to wavelength remains the same.

It can be shown that the discrepancies in the values of ϵ' [10] for fresh water are relatively small and amount to 2.5-3 percent; for the loss tangents, these differences are somewhat higher -- about 10-30 percent. The strongest differences are observed in the electrical characteristics of sea water of high salinity (40 percent) -- for the dielectric constant the results differ by 20-30 percent, and $\text{tg } \delta$ -- by nearly twofold.

2. Review of Experimental Data on the Electrical Characteristics of Water

We begin this section with a comparison of the calculation made and available experimental data in the decimeter and meter wavelength ranges for fresh water. These data are taken mainly from a detailed handbook by Ya. Yu. Akhrodov [9] and a recent review [4].

From an examination of the data shown in Figs. 3 and 4, where the results of calculating ϵ' and $\operatorname{tg} \delta$ for fresh water (on an altered scale with respect to Figs. 1 and 2) and experimental data from the studies [16-23] are presented, we can conclude that there is good agreement between the results of calculation based on the Debye model for fresh water in the decimeter range. For most experimental points of ϵ' , the agreement with the calculated curve is better than 0.3 percent, and only four experimental points have a nonagreement with the calculated curve of the order of 1 percent.

Experimental investigations of the dielectric constants of sea water, an electrolytic solution of the salts of Na, K, Ca, Mg, Ba, and other elements, are few and contradictory.

An important, but little-studied problem in the investigation of the electrical characteristics of sea water is the problem of the effect of salts, besides sodium chloride, on the dielectric properties⁴. [11]

Very recently, as part of an investigation of the possibilities of the remote probing of the ocean surface, a detailed study was made [8] of the dielectric characteristics of sea water samples taken from different parts of the World Ocean and solutions of various concentrations in the 11 cm range.

From an inspection of Figs. 5 and 6 (the argument of the graphs is the weight concentration of sodium chloride in the solutions [8]), it is clear that the dielectric constant of sea water ϵ'_M is smaller than the dielectric constant of a sodium

⁴ On the average, sea water with a salinity of 35 per mill contains the following [14, 5]: NaCl -- 27.2 g per kg of water; MgCl₂ -- 3.8 g; MgSO₄ -- 1.7 g; CaSO₄ -- 1.2 g; K₂SO₄ -- 0.9 g; CaCO₃ -- 0.1 g; other compounds present in the water of oceans are contained in very small amounts.

chloride solution of the same concentration as the sea water, ϵ'_{NaCl} , for all salinity values.

The dielectric constant of tap water differs from the ϵ' of distilled water only slightly -- by a relative value of about 0.3 percent; and the losses are virtually the same for these types of fresh water.

These graphs enable us to examine an experimentally important problem, the validity of the modeling of sea water with a sodium chloride solution.

The real part of the dielectric permittivity ϵ'_M of sea water with a salinity of 35 per mil, containing 27.2 g per kilogram of sodium chloride solution is smaller than the ϵ'_{NaCl} of an NaCl solution containing 27.2 g/kg of this salt, by a relative value of about 0.5 percent (0.4 unit of the mean value of $\epsilon' = 80$) and, /12 if we are concerned with experiments, where the relative precision in the determination of about 0.5 percent does not play a role, the modeling of sea water with the corresponding solution of NaCl can solve the problem posed.

If in the experiments we use a sodium chloride solution with a concentration of 35 g per kg of solution, the relative error in the determination of ϵ' will be positive and amount to about 2 percent (about 1.5 units of the mean value $\epsilon' = 80$). When it is necessary to reduce these errors, sea water must be modeled with a 35 per mil NaCl solution having a concentration of 29.5 g/kg, as follows from the experimental plots.

As far as the losses are concerned (Fig. 6), ϵ''_M differs from the ϵ''_{NaCl} of the sodium chloride solution (with a concentration corresponding to the NaCl concentration in sea water) by about 4 percent (salinity is 35 per mil), and the error here rises with increase in salinity.

When an NaCl solution with a concentration of 35 g per kg of solution is used, the losses in this solution will be much higher than in sea water with a 35 per mil salinity, by about 15 percent.

All the foregoing pertains to the 11 cm range. In the shorter-wavelength range, the difference in the electrical characteristics of solutions of electrolytes will be reduced, as is also true of the effect of the different chemical composition of the electrolyte. In the decimeter and meter ranges, the tendency is the reverse and the problem of modeling sea water with a sodium chloride solution when analyzing electrical characteristics must be solved experimentally.

We once again note that in the related calculations and graphs of the studies [7,12,13], in the present study by salinity (in ppt [parts per thousand] is meant only the presence of sodium chloride in the solutions. And if we discuss the high precision with which the calculations of the dielectric parameters (up to 13 0.1 percent) were made ([7]), then with reference to the above-expressed considerations, it must be stated that the salinities of the sodium chloride solution do not correspond to the salinities of sea water, in contradiction to the assertions of the authors of this study concerning the negligible effect of other salts on the electrical parameters of sea water. Still, generally speaking, at each wavelength one can find a definite correspondence between the salinity of sea water and the salinity of the sodium chloride solution in the sense of the identity of their electrical parameters. For example, from Fig. 5 it follows that sea water with a 35 per mil salinity has virtually the same electrical parameters at a wavelength of 11 cm as a sodium chloride solution with a concentration of about 29.5 g/kg (or 29.5 per mil).

3. Radiation Characteristics and Radiobrightness Temperature of Water Surface

The emissivities of a smooth water surface with vertical ϵ_v and horizontal ϵ_h polarization, and the coefficient of polarization P are given by the following expressions:

$$\epsilon_v = \frac{4(\epsilon' a + \epsilon'' b) \cos \theta}{|\epsilon|^2 \cos^2 \theta + 2(\epsilon' a + \epsilon'' b) \cos \theta + a^2 + b^2}, \quad (5)$$

$$\epsilon_h = \frac{4a \cos \theta}{(\cos^2 \theta + a)^2 + b^2}, \quad (6)$$

$$P = \frac{\epsilon_v - \epsilon_h}{\epsilon_v + \epsilon_h}, \quad (7)$$

$$a = \frac{\sqrt{2}}{2} \{[(\epsilon' - \sin^2 \theta)^2 + \epsilon''^2]^{1/2} + \epsilon' - \sin^2 \theta\}^{1/2}, \quad (8)$$

$$b = \frac{\sqrt{2}}{2} \{[(\epsilon' - \sin^2 \theta)^2 + \epsilon''^2]^{1/2} - \epsilon' + \sin^2 \theta\}^{1/2}, \quad (9)$$

where θ is the angle of observation, measured from the vertical, [14]

ϵ_v , ϵ_h , and P are functions of temperature t, salinity S, angle of observation θ , and radiation wavelength λ .

The radiation characteristics of a smooth water surface, calculated by Eqs. (5) - (9) for different temperatures, salinities, and angles of observation are represented by a series of graphs in Table 4 ⁵.

To estimate the penetrating power of passive probing, the coefficient of absorption Q and the "effective depth" L were calculated, where a 90 percent radiothermal radiation of the layer was formulated:

$$Q = 2\pi \frac{8.7}{\lambda} \left[\frac{\epsilon'(\sqrt{1 + \epsilon''^2} - 1)}{2} \right]^{1/2} \quad (\text{db/m}) \quad (10)$$

$$L = \frac{19.1}{Q} \quad (\text{m}) \quad (11)$$

⁵ The discrepancies with the data in [12], for reasons given above, are from 2 per mil (fresh water) to 25 per mil (salt water) for emissivity, for a zero angle of observation.

In the wavelength range $\lambda = 8.5-200$ cm (Figs. 7 and 8), the value falls off with increase in wavelength at all temperatures and salinities. And for fresh water this decline is more pronounced and is exponential in character:

$$Q \sim \lambda^{-2}$$

For fresh water, Q decrease with rise in temperature, while for salt water it rises, at the same salinities. With increase in salinity at a fixed temperature, the coefficient of absorption rises. All these changes in Q for salt water do not exceed one order throughout this wavelength range. The values of Q and L for $\lambda = 18, 75$, and 200 cm are given in Table 2.

/15

From Table 3 it follows that in the range $\lambda = 18$ cm radiation is formed in the fresh water layer 8.5 cm thick, and for $\lambda = 75$ cm -- in the layer 1.5 to 5.2 m thick (with variation in t from 0 to 40° C). For salt water, the layer forming the radiation extends in depth from 1 to 5 cm (depending on temperature).

Fig. 9 presents the results of the calculation of the emissivity ϵ of a smooth water surface in the range from 3 mm to 200 cm, the temperature range (0-40° C), and the salinity range (0-40 per mil).

From an examination of the graphs, it follows that in the frequency dependence of ϵ there are two wavelength ranges, appreciably differing in the effect of temperature and salinity on ϵ . The boundary (provisionally) lies at about 5-7 cm. Below this value the emissivity is virtually independent of salinity, in general, and with increase in temperature the value of ϵ substantially decreases. This range is regarded as promising from the standpoint of the remote determination of the surface temperature of the World Ocean [24].

In the decimeter and meter ranges, salinity strongly affects ϵ , and with increase in the working wavelength the effect of

salinity increases. This is physically associated with a sharp rise in the loss tangent in the decimeter and meter ranges (see Section 2).

The emissivity of fresh water, as can be seen from the graph, in general does not depend on wavelength owing to the absence of the frequency dispersion of the dielectric constant and the smallness of the loss tangent.

The radiobrightness temperature curves are shown in Fig. 10. The trend of these curves in general is analogous to the curves of the emissivities (Fig. 9). Even though here there are several 16 features, for example, in the wavelength range $\lambda = 20$ cm, the curves for the various salinities intersect and change their temperature dependence. The radiobrightness temperatures of fresh water comprise the range $95-115^{\circ}$ K in the decimeter wavelengths. With increase in wavelength (especially in the meter range), there is a drop in the radiobrightness temperatures of sea and fresh water and it is of the order of 80° K ($\lambda = 100$ cm, $t = 40^{\circ}$ C); with decrease in surface temperature, this drop becomes smaller at each wavelength.

The dependence of the emissivity of a water surface on angle of observation is shown in Fig. 11. Due to the large electrical losses, the emissivity differs quite appreciably from unity near Brewster's angle. However, the value of this angle remains nearly the same as for fresh water, as for sea water; it is about $83-85^{\circ}$, independently of the radiation wavelength.

The temperature characteristics in this range are quite unusual. For example, in Fig. 12 are constructed the temperature functions at the wavelength 18 cm (angle of observation is the nadir). From these graphs it is clear that for fresh water there is a positive gradient of ϵ with respect to temperature; for salt water (40 per mil) there is a large negative gradient; and for water with a salinity of 20 per mil, generally the temperature

dependence of emissivity is absent. From these graphs it is also clear that for any working wavelength it is possible to find the salinity for which the dependence of ϵ on temperature will be absent. We note that we are discussing emissivity, while the situation is otherwise for radiobrightness temperatures. For example, in the case present for water with 20 per mil salinity T_{br} at 40° C is higher than at 0° C, though the emissivity remains 17 unchanged (Fig. 12).

Analogous curves are shown in Fig. 13 for the radiation wavelength 75 cm.

Since the quiet water surface is used for calibrating the radiometric temperature, we must take into account these features of the temperature dependence of the radiobrightness temperature of water with varying salinity. Similar features are absent in the centimeter and millimeter ranges.

Figs. 14 and 15 present graphs of the dependence of emissivity and radiobrightness temperature (at the nadir, $\theta = 0^{\circ}$) on salinity for a number of wavelengths: 18 cm, 75 cm, and 200 cm. Common to these curves for the decimeter and meter wavelengths is a decrease in emissivity and in radiobrightness temperature with increase in water salinity, where this reduction is nonlinear especially in the meter wavelength range.

In addition, temperature has a fairly strong effect: at the wavelength of 18 cm and at 0° C, in general there is no effect of salinity on ϵ ; at 0° C, the drop in the value of ϵ with variation from 0 to 40 per mil is 0.04 (Fig. 14). With increase in the working wavelength, the drop in emissivity increases also for $\lambda = 75$ cm and 200 cm, being ($t = 20^{\circ}$ C) approximately 0.17 and 0.25, respectively.

The drop in radiobrightness temperature ΔT_{br} with variation in salinity from 0 to 30 per mil is as follows (Fig. 15):

$t^{\circ}\text{C}$	$\lambda=18\text{ cm}$	$\lambda=75\text{ cm}$
0	0°K	20°K
20	5°K	50°K
40	18°K	62°K

For the normalized sensitivity of the radiometric system of 18 the order of about 0.4°K , the number of gradations when salinity is varied from 0 to 30 percent at $t = 20^{\circ}\text{C}$ is $2 - 3 \text{ m} \sim 25$ [sic] at wavelengths of 18 cm and 75 cm, respectively.

However, as follows from these figures, with increase in λ there is a rise in the nonlinearity of the functions, and a rapid change in χ , as well as in T_{br} is observed in the salinity ranges from 2-5 per mil to 25-25 per mil with a subsequent abrupt drop in the gradient of χ as a function of S . Therefore, the first recommendation in the investigation of salinity can be seas with low salinity, for example, the Baltic or Black seas, and also regions of the flow of rivers into an ocean.

It should be noted that temperature strongly affects (Fig. 15) the gradient of T_{br} as a function of S in the region where there is no linearity of this function (up to salinities of the order of 20-25 per mil).

$\lambda=18\text{ cm}$		$\lambda=75\text{ cm}$	
$t^{\circ}\text{C}$	$\frac{\partial T_{\text{br}}}{\partial S} \text{ }^{\circ}\text{K}/\text{‰}$	$t^{\circ}\text{C}$	$\frac{\partial T_{\text{br}}}{\partial S} \text{ }^{\circ}\text{K}/\text{‰}$
0	0	0	1
20	0.25	20	2
40	0.5	40	3.5

We note that when interpreting experimental material, one must know the thermodynamic temperature of the surface. Investigation of the salinity dependence of polarization characteristics revealed the following.

The sensitivity of the radiation characteristics to the salinity of two polarizations substantially depends on the type of polarization, where for vertically polarized radiation this characteristic increases with respect to the analogous quantity for observations at the nadir. For $t = 20^{\circ} \text{ C}$ and salinity change from 0 to 40 per mil, the change in the radiobrightness temperature when observations are made of vertically polarized radiation ^{/19} ($\theta = 30^{\circ}$), the ΔT_{br} for $\lambda = 18 \text{ cm}$ and 75 cm is 13° K and 60° K , respectively (Fig. 15a).

From this it is clear that observation of vertically polarized radiation ($\theta = 30^{\circ}$) yields an advantage in particular in the meter wavelength range, though not very substantial. With an increase in the angle of observation to $\theta = 60^{\circ}$, the advantage in the contrast ΔT_{br} of vertically polarized radiation compared with observations at the nadir can be up to 1.7 times in the meter range.

The sensitivity of the value of x_h of horizontally polarized radiation to salinity decreases with increase in the angle of observation and, evidently, is not of special interest for the problems considered here.

Polarization Characteristics

By analyzing the graphs (Figs. 16, 17, 18) which present the angular dependence of the coefficient of polarization (P) and the frequency dependence of P , we should note an important feature of the polarization measurements: weak dependence over the entire wavelength range of the coefficient of polarization on the water surface temperature (see also Table 4).

The dependence of P on salinity is also relatively weak, with a slow rise in the effect of salinity on the coefficient of polarization in the meter range. Thus, for $\theta = 30^{\circ}$, $t = 20^{\circ} \text{ C}$, and a salinity change from 0 to 40 per mil, P changes (in absolute

value) by 0.4 percent ($\lambda = 18$ cm), 1.6 percent ($\lambda = 75$ cm), and 2.2 percent ($\lambda = 200$ cm) (Fig. 18).

When the angle of observation is decreased, the change of P in the meter range does not exceed 8 percent in absolute magnitude ($\theta \leq 60^\circ$, $t = 40^\circ$ C, $\lambda = 200$ cm).

Experimental Results

/20

There have been virtually no special studies of the radiation characteristics in the decimeter and meter range in the temperature and salinity ranges, however, the theoretical possibility of distinguishing different degrees of salinity from radiobrightness temperature observations was shown [25,26]. Using an airborne passive radar in the wavelength 21 cm, profiles of the salinities of several routes were obtained during a flight over the mouth of the Mississippi River (estuary) into the Gulf of Mexico. After computer processing of the results, to reduce the redundancy color profiles of salinity (four gradations) from fresh to sea water were constructed.

The sensitivity of ΔT_{br} to salinity was about 1° K per 1 per mil change in salinity.

Nonetheless, the profiles found appreciably supplement maritime maps of the distribution of the salinity of this estuary.

The question of modeling sea water with different salt concentrations with NaCl solution in measuring the radiation characteristics is essentially, particularly in the experimental aspect. From an inspection of the function $\alpha = \alpha(\epsilon, \epsilon'')$ (when $\theta = 0^\circ$), the coefficients $\left. \frac{\partial \alpha}{\partial \epsilon} \right|$ and $\left. \frac{\partial \alpha}{\partial \epsilon''} \right|$ are $1.5 \cdot 10^{-3}$ and $1 \cdot 10^{-3}$ unit of measurement per unit of change in ϵ' or in ϵ'' in the range $\epsilon, \epsilon'' \sim 80$. It can be shown that in the range $\lambda = 11$ cm the absolute difference of the radiation characteristics of an NaCl solution containing 35 g salt per kg of solution and of sea water with 35 per mil salinity (see Section 2) is of the order of about

$1.3 \cdot 10^{-2}$, and the corresponding difference in the radiobrightness temperature (for $T_0 = 300^\circ \text{ K}$) is $3-4^\circ \text{ K}$.

Interestingly, this difference is composed mainly of a change /21 in the quenching of the NaCl solution and of actual sea water.

In the shorter wavelength range, apparently the difference in the radiation characteristics of these electrolytes decreases, while in the longer wavelength range the situation is the reverse, and for a sufficiently high precision in the measurement of radiobrightness temperatures, the modeling of sea water with an NaCl solution (of the same salinity) is not applicable.

Further experiments must show the degree of the dependence of the radiation characteristics of an electrolyte on its chemical composition.

4. Allowing for Atmospheric Glow

In view of the significant dependence of the coefficient of reflection of a water surface on frequency, allowance for atmospheric glow (atmosphere and cosmic noise) can substantially modify the above-presented ratios of radiobrightness temperatures.

The radiobrightness temperature, measuring with a radiometric system, in general is as follows (without allowing for attenuation in the atmosphere and the averaging action of the antenna radiation pattern) /6,27/:

$$T_{br\ j} = \epsilon_j T_0 + T_{Hj}^{\circ} \quad (12)$$

where $i, j = v, h$ -- (vertical and horizontal polarizations),

ϵ_j = emissivity,

T_{Hj} = atmospheric glow reflected from the Earth's surface,

which is:

$$T_{Hj}^{\circ} = \frac{1}{4\pi} \int_0^{2\pi} \int_0^{\pi/2} (\epsilon_{jM} + \epsilon_{jH}) T_0(\theta') \sin \theta' d\theta' d\varphi' \quad (13)$$

where $T_H(\theta)$ is the radiobrightness temperature of the atmosphere, and /22

$\gamma_{ji}(\theta, \theta', \varphi')$ are the coefficients of surface scattering: here

$$\alpha_j = 1 - \frac{1}{4\pi} \int_0^{2\pi} \int_0^{\pi/2} (\gamma_{jv} + \gamma_{jn}) \sin \theta' d\theta' d\varphi' \quad (14)$$

Since the quiet water surface is a virtually mirror surface in the ranges considered, that is, $\gamma_{ji} = \delta(\theta - \theta') \delta(\varphi - \varphi')$, in other words, the coefficients γ_{ji} are delta functions, Eq. (12) becomes simplified:

$$T_{brH} = \alpha_j T_0 + (1 - \alpha_j) T_H. \quad (15)$$

When measuring radio emission from rough surfaces (wave-tossed sea and solid surface), especially at grazing angles of observation ($\theta > 60^\circ$) in ground surface experiments, allowance for glow must be made with reference to the complete expressions Eqs. (12) - (14) and the distribution of atmospheric temperature [7], and the averaging action of the antenna radiation pattern⁶.

Not being sufficiently exact, Eq. (15) nonetheless gives the first order of correction to the effects of glow caused by atmospheric radiation and in the meter range can qualitatively alter the functions under discussion, since the brightness temperature of the atmosphere in this range is 20-50° K [28].

With reference to Eq. (15) and the averaged radiobrightness temperature of the atmosphere in the decimeter and meter ranges [28] and in the millimeter and centimeter ranges (for the model of the atmosphere with content of precipitable water $1 \cdot 10^{-2}$ cm)

⁶ As shown by experiments [30], these effects are considerable even at angles of observation larger than 50-60° with an antenna that has a pattern of about 10°.

[29]; Fig. 19 presents the radiobrightness temperature curves for the water surface. As can be seen from comparing Fig. 10 and [23] Fig. 19, the effect of atmospheric glow on these functions is substantially. Namely, even at wavelengths > 1 m a sharp rise in the radiobrightness temperature of the water surface is observed, independently of its thermodynamic temperature and the salinity, which is related to a rise in the noise temperature of the atmosphere in this range. And the $T_{br,H}$ of salt water (40 per mil) is $80-90^\circ$ for the 1 m wavelength, while this quantity, without allowing for glow, T_{br} , is $40-50^\circ$ K (Fig. 10). From Fig. 19 there follows the important conclusion that the optimal range when one investigates the salinity of sea water by remote methods is the 50-80 cm wavelength range. With a further increase in the wavelength, the dependence of $T_{br,H}$ on salinity falls off quite rapidly. The values of $T_{br,H}$ in the above-indicated range lies in the range 75-135 for fresh and for salt water.

Figs. 20, 21, and 22 are detailed curves of the radiobrightness temperature with allowance for atmospheric glow as a function of salinity and the thermodynamic temperature of the water surface at the wavelengths 18 and 75 cm.

The examination of the effect of salinity on the trend of the T_{br} curves (Fig. 20) shows that glow increases absolutely the value of the radiobrightness temperature by not more than $3-5^\circ$ K (wavelength 18 cm) and approximately by 20° K for $\lambda = 75$ cm (see Fig. 20 and Fig. 15). And in the former case the nonlinear dependence of the radiobrightness temperature with variation in salinity in general is retained, while in the latter case -- some change in its character takes place. Especially at the radiation wavelength of 75 cm the boundary of the abrupt decrease in the gradient $\Delta T_{br,H} / \Delta S$ shifts toward the 10 per mil salinity range ($t = 40^\circ$ C). The analogous boundary without allowing for the glow $\Delta T_{br} / \Delta S$ lies in the region of 20-25 per mil salinity ($t = 40^\circ$ C). This circumstance confirms the earlier-made

conclusion of the utility of investigations of low salinities (from 10 to 12 per mil) by remote methods at the working wavelength of 75 cm.

The gradients $\Delta T_{br,H} / \Delta S$ and $\Delta T_{br} / \Delta S$ (Figs. 20 and 15) in the salinity range 0-20 per mil at the wavelength 18 cm show nearly no change (see Section 3); at $\lambda = 75$ cm in the 0-10 per mil range, $\Delta T_{br,H} / \Delta S$ is 3.5° K/l per mil when $t = 40^\circ \text{ C}$, and further, 0.8° K/l per mil (15-40 per mil) (compare Section 3).

The effect of the noise temperature of the atmosphere in the temperature dependence of $T_{br,H} (T_0)$ (Figs. 21 and 22) reduces to an increase in the absolute radiobrightness temperatures of not more than 8 and 20° K (at $\lambda = 18$ and 75 cm, respectively). The nature of the curves remains virtually unchanged (compare Figs. 21 and 12, and Figs. 22 and 13).

The general trend is one of a rise in the negative gradient $\Delta T_{br,H} / \Delta S$ with rise in salinity, especially at the wavelength 75 cm, though for fresh water this gradient is always positive. At the salinity $S = 40$ per mil and $\lambda = 18$ cm, the temperature function is virtually not observed.

5. Coefficient of Reflection from Water Surface. Experimental Data

Owing to developments in the possible application of radar systems in the decimeter and meter ranges for determining the parameters of the water surface (for example, illegible), it is of interest to investigate the problem of the dependence of the coefficient of reflection (with respect to thickness) in this range on the thermodynamic temperature and on salinity.

The coefficient of reflection with respect to thickness can be found from the relations (5) and (6) given the condition (see Section 4) that

$$|R|^2 = 1 - \alpha. \quad (16)$$

From an inspection of Fig. 23, where the frequency functions /25 (for observations at the nadir) are given for the temperatures of 0, 20, and 40° C and the salinities of 0, 20, and 40 per mil, it is clear that in the centimeter range the coefficient of reflection increases with increase in wavelength, there is no dependence on salinity, and a unique dependence on temperature (for wavelength of 5-7 cm) is observed -- the higher the temperature, the higher the coefficient of reflection.

In the decimeter and meter ranges, the dependence on wavelength for fresh water is absent, while the dependence on temperature is an inverse one -- the higher the temperature, the lower the coefficient of reflection. And the radiation wavelength has nearly no effect on the gradient $\Delta IRI^2 / \Delta T_0$, which is a value of $6 \cdot 10^{-2}$ percent per degree of temperature change.

For fresh water at all salinities, the coefficient of reflection is higher than for fresh water. The temperature gradient for sea water can be either negative, or positive, depending on salinity. More detailed temperature curves and salinity functions can be obtained from data shown in Figs. 12 and 14 ($\lambda = 18, 75$ cm) or from Table 4 with reference to Eq. (16).

Experimental data. Published experimental results on the measurement of the coefficient of reflection in a wide frequency range are relatively few.

The study /31/ presents the results of measuring the IRI of an open surface of fresh water in the centimeter range over a wide range of temperatures. Fig. 24 gives the results of calculations of temperature functions at the frequencies of 13.7 and 22.2 GHz and experimental points at the frequencies 19, 24, and 22.43 GHz.

From a comparison of these results it is clear that the differences in the ranges 1.6 and 1.35 cm are about 0.25 percent and about 1 percent, respectively. This difference evidently was caused by the nonagreement of experimental and calculation frequencies. /26

Of major interest is a study [32] in which are presented experimental frequency characteristics of IRI^2 of fresh and sea water in the wide frequency range from 0.1 to 4 GHz, where in the 2.5-4.0 GHz measurements were made with a sweep generator from the open water surface, and a special coaxial chamber for water was designed for the 0.1-2 GHz range.

In the low-frequency range the calculated curves (dashed) agree well with the experimental points for the same salinity values (Fig. 24).

The results obtained in the 2.5-4.0 GHz range raise doubt, since the coefficient of reflection throughout nearly the entire range is smaller for sea water than for fresh.

In addition, the burst in the value of IRI^2 at about the frequency 3 GHz is doubtful.

The very authors of this experiment [32] regard the experimental results in this range as well as the features noted to be insufficiently exact to draw conclusions on the features of the electrical properties of salt water.

The conclusions on the possibility of modeling sea water with an NaCl solution by comparison with data from measurements of radiation characteristics, given in Section 3, are fully valid also when compared with experimental data on reflection characteristics.

From these calculations made with the experimental data it can be concluded that the use of the frequency range below 1 GHz is effective for the purposes of detecting and measuring the salinity of the water surface in the active measurement mode.

Conclusions

Based on the above-given results the following conclusions can be drawn.

[27]

1. There is no well-defined frequency dependence of the dielectric constant in the decimeter and meter ranges. Owing to the presence of a high specific conductivity of sea salts, the loss tangent in the decimeter and meter ranges rises sharply, while for fresh water, the loss tangent decreases linearly in the 1-200 cm range. The values of ϵ' and $\text{tg } \delta$, calculated for fresh water, agree well with available extensive experimental material, which enables us to evaluate the validity of the Debye polarization model for fresh water in the UHF range.

Experimental data on the electrical characteristics of sea water are scanty, therefore a definitive decision on the correspondence of the Debye dispersion model for solutions of electrolytes in the low-frequency range is a matter for the future.

2. The emissivity of fresh water at wavelengths longer than 10 cm is virtually independent of frequency for a fixed water surface temperature. The emissivity of sea water falls off with increase in wavelength and in salinity. The coefficient of polarization depends weakly on temperature and salinity in the decimeter and meter ranges.

3. Atmospheric glow delimits on the long-wave side the range of wavelengths which can be used for remote probing using passive measurements of wavelengths of the order of 1-2 m.

The presence of atmospheric glow substantially reduces the sensitivity of the radiobrightness temperature toward a change of both the thermodynamic temperature and of salinity. /28

4. The 3-8 cm wavelength range can be recommended for the measurement of the surface temperature by passive remote methods.

But for investigating salinity, the most advantageous is the 50-80 cm range (with reference to atmospheric glow) with the detection predominantly of vertically polarized radiation.

When 0.3 (0.8) and 18 cm range radiometric systems are available, the temperature fields of a smooth water surface (first wavelength) and the salinities (with reference to temperature) can be measured from data at the second wavelength on the gradient of the radiobrightness temperature per unit change in salinity of 0.3-0.5° K.

Selection of the optimal wavelength depends on the irradiated salt concentrations. Thus, passive methods can be recommended for seas with weak salinity or for regions in which rivers flow out into the ocean.

5. Experimental data on the coefficient of reflection with respect to thickness in the low-frequency range (100 MHz - 2 GHz) agree with the calculated functions for the same salinities and thermodynamic temperatures.

Use of the low-frequency UHF range (below 1 GHz) is desirable for investigating the distribution of salinity by active remote methods.

In selecting the wavelength for probing, the resolving power with increase in wavelength must be taken into account.

An examination is made of the effect of sea water temperature /29 and salinity on its dielectric constants and the radiation characteristics of a smooth water surface in the 10-200 cm wavelength range. With reference to the dependence of dielectric constants on temperature and salinity, and also the effect of atmospheric glow, it was shown that the optimal working range of working wavelengths for investigating the distribution of the salinity of an ocean by remote passive methods is the 60-80 cm range. And corresponding to a salinity change from 0 to 30 per mil is a 43.5°K decrease in the radiobrightness temperature at the wavelength 75 cm, when the temperature of the radiating surface is 20° C.

Experimental material was compared with theoretical calculations.

TABLE 1. ELECTRICAL CHARACTERISTICS OF FRESH AND SEA WATER

$t^{\circ}\text{C}$	ε' ε''	$S\%$	λ cm								
			10	18	21	30	50	75	100	150	200
0	ε'	0	79.45	85.33	86.07	86.93	87.70	87.70	87.70	87.70	87.70
		20	74.53	79.52	80.09	81.06	81.59	81.82	81.82	81.90	81.90
		40	68.70	73.08	73.62	74.43	74.92	75.12	75.12	75.20	75.20
	ε''	0	0.314	0.174	0.148	0.105	0.063	0.042	0.031	0.021	0.016
		20	0.429	0.379	0.387	0.443	0.626	0.885	0.156	0.705	2.263
		40	0.565	0.619	0.667	0.842	1.289	1.876	2.481	3.692	4.913
10	ε'	0	79.90	82.87	82.87	83.70	83.70	83.70	83.70	83.70	83.70
		20	74.65	77.19	77.47	77.98	78.19	78.34	78.34	78.34	78.34
		40	68.48	70.66	70.91	71.30	71.51	71.64	71.64	71.64	71.64
	ε''	0	0.222	0.124	0.107	0.074	0.045	0.030	0.022	0.015	0.011
		20	0.383	0.411	0.441	0.552	0.841	1.224	1.613	2.403	3.196
		40	0.572	0.754	0.838	1.120	1.786	2.639	3.503	5.238	6.977
20	ε'	0	77.76	79.20	80	80	80	80	80	80	80
		20	72.83	74.15	74.36	74.51	74.71	74.78	74.78	74.78	74.78
		40	66.43	67.58	67.70	64.89	68.01	68.08	68.08	68.08	68.08

TABLE 1 [Conclusion]

$t^{\circ}\text{C}$	ε' ε''	$S\%$	λ cm								
			10	18	21	30	50	75	100	150	200
30	ε''	0	0.167	0.093	0.078	0.055	0.033	0.022	0.017	0.011	0.0082
		20	0.374	0.466	0.515	0.679	0.072	1.577	2.094	3.126	4.164
		40	0.621	0.914	1.039	1.427	2.318	3.448	4.588	6.869	9.155
	ε'	0	75.74	76.50	76.50	76.50	76.50	76.50	76.50	76.50	76.50
		20	70.12	70.89	71.03	71.16	71.22	71.22	71.22	71.22	71.22
		40	63.65	64.28	64.34	64.46	64.52	64.52	64.52	64.52	64.52
	ε''	0	0.126	0.07	0.061	0.042	0.025	0.017	0.013	0.0085	0.0064
		20	0.388	0.541	0.610	0.827	1.334	1.979	2.631	3.937	5.245
		40	0.698	1.105	1.269	1.768	2.904	4.338	5.776	8.654	11.54
	ε'	0	72.47	73.20	73.20	73.20	73.20	73.20	73.20	73.20	73.20
		20	66.98	67.47	67.53	67.59	67.66	67.66	67.66	67.66	67.66
		40	60.47	60.85	60.85	60.89	60.96	60.96	60.96	60.96	60.96
40	ε''	0	0.10	0.056	0.048	0.034	0.020	0.013	0.010	0.0067	0.0051
		20	0.426	0.642	0.732	0.012	1.649	2.459	3.272	4.90	6.531
		40	0.819	1.356	1.566	2.202	3.638	5.444	7.252	10.87	14.49

TABLE 2. ELECTRICAL CHARACTERISTICS OF FRESH AND SEA WATER

λ cm	ϵ' ϵ''	$t^\circ C$	% salinity								
			0	5	10	15	20	25	30	35	40
18	ϵ' ϵ''	0	85.33	83.14	82.25	80.39	79.52	78.45	76.09	74.15	73.08
			0.174	0.223	0.273	0.331	0.379	0.430	0.493	0.558	0.619
	ϵ' ϵ''	20	79.20	79.93	78.15	76.07	74.15	72.19	70.28	68.29	67.58
			0.093	0.176	0.266	0.362	0.466	0.562	0.681	0.791	0.914
	ϵ' ϵ''	40	73.20	73.30	71.21	69.31	67.47	66.61	64.72	62.78	60.85
			0.056	0.186	0.322	0.484	0.642	0.792	0.962	1.144	1.356
75	ϵ' ϵ''	0	87.70	85.71	84.72	82.72	81.82	80.72	78.22	76.22	75.12
			0.042	0.241	0.450	0.694	0.885	1.099	1.362	1.633	1.876
	ϵ' ϵ''	20	80	80.60	78.80	76.70	74.78	72.80	70.80	68.80	68.08
			0.022	0.384	0.763	1.164	1.577	1.997	2.497	2.962	3.448
	ϵ' ϵ''	40	73.20	73.50	71.40	69.50	67.66	66.80	64.90	62.9	60.96
			0.013	0.575	1.146	1.823	2.459	3.109	3.822	4.588	5.444
200	ϵ' ϵ''	0	87.70	85.80	84.80	82.80	81.90	80.80	78.30	76.30	75.20
			0.016	0.547	1.105	1.753	2.263	2.836	3.538	4.260	4.913
	ϵ' ϵ''	20	80	80.60	78.80	76.70	74.78	72.80	70.80	68.80	68.08
			0.008	0.976	1.987	3.051	4.164	5.281	6.617	7.854	9.155
	ϵ' ϵ''	40	73.20	73.50	71.40	69.50	67.66	66.80	64.90	62.90	60.96
			0.005	1.506	3.029	4.837	6.531	8.266	10.172	12.213	14.49

TABLE 3. ATTENUATION AND EFFECTIVE LAYER OF FRESH AND SEA WATER

$t^\circ C$	% /100	$\lambda = 18$ cm		$\lambda = 75$ cm		$\lambda = 200$ cm	
		Q (dB/m)	L (m)	Q	L	Q	L
0	0	226	0.085	14.2	1.34	1.98	9.63
	20	502.8	0.038	207.9	0.071	211.9	0.09
	40	769.6	0.025	474.6	0.04	335.3	0.057
20	0	104.5	0.18	6.99	2.73	0.77	24.7
	20	593.2	0.032	415.4	0.046	302.3	0.063
	40	1046	0.018	684	0.028	456.7	0.042
40	0	58	0.33	3.69	5.18	0.58	32.6
	20	762.1	0.025	544.8	0.035	376.1	0.051
	40	1387	0.014	856.2	0.022	554.4	0.034

TABLE 4. RADIATION CHARACTERISTICS AND COEFFICIENT OF POLARIZATION OF FRESH AND SEA WATER

E	t°C	α_0	S%	λ cm		
				18	75	200
0	0	α_0	0	0,349	0,349	0,349
			20	0,349	0,302	0,209
			40	0,341	0,238	0,147
			0	0,362	0,362	0,362
			20	0,352	0,257	0,161
			40	0,323	0,185	0,112
	20	α_0	0	0,374	0,375	0,375
			20	0,349	0,202	0,134
			40			
			0			
			20			
			40			

TABLE 4 /CONTINUATION/

S	t°C	α_h, α_v	S%	λ cm		
				18	75	200
10	0	α_h	0	0,345	0,344	0,344
			20	0,344	0,297	0,207
			40	0,336	0,234	0,145
		α_v	0	0,354	0,353	0,352
			20	0,353	0,305	0,213
			40	0,345	0,241	0,149
		P	0	0,012	0,012	0,012
			20	0,012	0,013	0,014
			40	0,012	0,013	0,014
	20	α_h	0	0,358	0,357	0,357
			20	0,347	0,253	0,159
			40	0,319	0,182	0,110
		α_v	0	0,367	0,366	0,366
			20	0,355	0,280	0,163
			40	0,327	0,187	0,114
		P	0	0,012	0,012	0,012
			20	0,012	0,013	0,014
			40	0,012	0,014	0,014
	40	α_h	0	0,370	0,370	0,370
			20	0,345	0,216	0,132
			40	0,294	0,152	0,092
		α_v	0	0,379	0,379	0,379
			20	0,354	0,222	0,136
			40	0,301	0,156	0,095
		P	0	0,012	0,012	0,012
			20	0,012	0,014	0,014
			40	0,013	0,014	0,015

TABLE 4 /CONTINUATION/

θ	$t^{\circ}C$	α_{h-v}	$S\%$	cm		
				18	75	200
20	0	α_h	0	0.332	0.332	0.332
			20	0.331	0.286	0.198
			40	0.324	0.225	0.130
		α_v	0	0.367	0.366	0.300
			20	0.366	0.317	0.222
			40	0.358	0.251	0.156
		ρ	0	0.050	0.050	0.050
			20	0.050	0.052	0.055
			40	0.050	0.054	0.057
	20	α_h	0	0.345	0.344	0.341
			20	0.334	0.243	0.152
			40	0.307	0.175	0.106
		α_v	0	0.380	0.380	0.380
			20	0.369	0.271	0.170
			40	0.340	0.196	0.119
		ρ	0	0.050	0.050	0.050
			20	0.050	0.053	0.057
			40	0.051	0.056	0.059
	40	α_h	0	0.357	0.357	0.357
			20	0.332	0.208	0.126
			40	0.282	0.145	0.088
		α_v	0	0.393	0.393	0.393
			20	0.367	0.232	0.142
			40	0.313	0.163	0.095
		ρ	0	0.050	0.049	0.049
			20	0.050	0.055	0.058
			40	0.052	0.057	0.059

TABLE 4 /CONTINUATION/

θ	$t^\circ\text{C}$	$\frac{\partial \rho}{\partial V}$	$S\%$	λ cm		
				18	75	200
30	0	α_h	0	0,311	0,310	0,310
			20	0,310	0,267	0,184
			40	0,303	0,209	0,129
		α_v	0	0,391	0,390	0,390
			20	0,390	0,339	0,238
			40	0,381	0,269	0,168
		ρ	0	0,114	0,114	0,114
			20	0,114	0,119	0,127
			40	0,115	0,125	0,132
	20	α_h	0	0,323	0,322	0,322
			20	0,313	0,227	0,141
			40	0,287	0,162	0,098
		α_v	0	0,405	0,404	0,404
			20	0,394	0,290	0,183
			40	0,363	0,210	0,128
		ρ	0	0,113	0,113	0,113
			20	0,114	0,123	0,131
			40	0,117	0,129	0,135
	40	α_h	0	0,334	0,334	0,334
			20	0,311	0,193	0,117
			40	0,263	0,135	0,082
		α_v	0	0,418	0,419	0,419
			20	0,391	0,249	0,153
			40	0,335	0,176	0,107
		ρ	0	0,112	0,112	0,112
			20	0,114	0,126	0,133
			40	0,119	0,131	0,136

TABLE 4 /CONTINUATION/

ϕ	$t^\circ\text{C}$	α, α_v	$S\%$	λ cm		
				18	75	200
40	0	α_h	0	0.281	0.280	0.280
			20	0.280	0.240	0.165
			40	0.273	0.188	0.115
		α_v	0	0.429	0.429	0.429
			20	0.428	0.374	0.264
			40	0.419	0.298	0.188
		P	0	0.209	0.209	0.209
			20	0.209	0.218	0.232
			40	0.211	0.228	0.241
	20	α_h	0	0.292	0.291	0.291
			20	0.283	0.203	0.126
			40	0.259	0.145	0.070
		α_v	0	0.444	0.443	0.443
			20	0.432	0.321	0.205
			40	0.399	0.234	0.144
		P	0	0.207	0.207	0.207
			20	0.209	0.225	0.239
			40	0.214	0.235	0.246
	40	α_h	0	0.302	0.302	0.302
			20	0.281	0.173	0.104
			40	0.237	0.120	0.074
		α_v	0	0.458	0.458	0.458
			20	0.429	0.276	0.171
			40	0.369	0.196	0.120
		P	0	0.205	0.205	0.205
			20	0.209	0.230	0.243
			40	0.218	0.240	0.248

TABLE 4 /CONTINUATION/

ϕ	$t^{\circ}\text{C}$	$\alpha_{\text{h}}, \alpha_{\text{v}}$	$S\%$	λ cm		
				18	75	200
50	0	α_{h}	0	0.242	0.241	0.241
			20	0.241	0.206	0.140
			40	0.235	0.160	0.097
		α_{v}	0	0.488	0.487	0.487
			20	0.407	0.428	0.307
			40	0.477	0.344	0.219
		P	0	0.338	0.338	0.338
			20	0.338	0.350	0.372
			40	0.340	0.365	0.366
	20	α_{h}	0	0.251	0.251	0.251
			20	0.243	0.174	0.107
			40	0.222	0.123	0.074
		α_{v}	0	0.504	0.503	0.504
			20	0.491	0.369	0.239
			40	0.455	0.272	0.169
		P	0	0.335	0.335	0.335
			20	0.337	0.361	0.383
			40	0.345	0.377	0.393
	40	α_{h}	0	0.261	0.261	0.261
			20	0.242	0.147	0.081
			40	0.203	0.102	0.061
		α_{v}	0	0.519	0.519	0.519
			20	0.488	0.319	0.199
			40	0.423	0.229	0.142
		P	0	0.331	0.331	0.331
			20	0.336	0.369	0.388
			40	0.351	0.364	0.397

TABLE 4 /CONTINUATION/

ϕ	$t^\circ\text{C}$	α_h, α_v ρ	$S\%$	λ cm		
				18	75	200
60	0	α_h	0	0.194	0.193	0.193
			20	0.193	0.164	0.111
			40	0.188	0.127	0.0766
		α_v	0	0.579	0.578	0.578
			20	0.578	0.513	0.375
			40	0.567	0.419	0.273
		ρ	0	0.499	0.499	0.499
			20	0.499	0.515	0.543
			40	0.502	0.535	0.561
	20	α_h	0	0.202	0.201	0.201
			20	0.195	0.138	0.0839
			40	0.177	0.097	0.058
		α_v	0	0.596	0.595	0.595
			20	0.582	0.447	0.296
			40	0.543	0.335	0.211
		ρ	0	0.494	0.494	0.494
			20	0.498	0.529	0.558
			40	0.507	0.551	0.571
	40	α_h	0	0.209	0.209	0.209
			20	0.194	0.163	0.092
			40	0.162	0.080	0.048
		α_v	0	0.612	0.612	0.612
			20	0.579	0.391	0.249
			40	0.507	0.284	0.178
		ρ	0	0.490	0.490	0.490
			20	0.499	0.540	0.565
			40	0.516	0.559	0.576

TABLE 4 /CONTINUATION/

			λ cm			
			18	75	200	
65	0	α_h	0	0.166	0.166	0.166
			20	0.166	0.141	0.095
			40	0.161	0.108	0.065
		α_v	0	0.643	0.642	0.642
			20	0.641	0.574	0.427
			40	0.630	0.474	0.314
		ρ	0	0.589	0.589	0.589
			20	0.589	0.606	0.637
			40	0.592	0.628	0.656
	20	α_h	0	0.173	0.173	0.173
			20	0.168	0.118	0.071
			40	0.152	0.083	0.049
		α_v	0	0.660	0.660	0.660
			20	0.645	0.504	0.339
			40	0.605	0.383	0.245
		ρ	0	0.584	0.584	0.584
			20	0.588	0.621	0.652
			40	0.598	0.645	0.667
40	α_h	0	0.180	0.180	0.180	
		20	0.166	0.099	0.059	
		40	0.139	0.068	0.041	
	α_v	0	0.676	0.677	0.677	
		20	0.642	0.443	0.287	
		40	0.567	0.326	0.207	
	ρ	0	0.579	0.579	0.579	
		20	0.588	0.634	0.660	
		40	0.607	0.654	0.672	

TABLE 4 /CONTINUATION/

θ	$t^{\circ}\text{C}$	$\alpha_{h,v}$	$S\%$	cm		
				18	75	200
70	0	α_h	0	0.137	0.137	0.137
			20	0.136	0.115	0.077
			40	0.133	0.089	0.053
		α_v	0	0.724	0.723	0.723
			20	0.723	0.653	0.500
			40	0.710	0.547	0.372
		ρ	0	0.682	0.682	0.682
			20	0.682	0.699	0.731
			40	0.685	0.721	0.750
	20	α_h	0	0.143	0.142	0.143
			20	0.138	0.096	0.058
			40	0.125	0.068	0.040
		α_v	0	0.741	0.740	0.741
			20	0.726	0.580	0.400
			40	0.664	0.449	0.293
		ρ	0	0.678	0.677	0.677
			20	0.680	0.714	0.746
			40	0.691	0.738	0.761
	40	α_h	0	0.149	0.149	0.149
			20	0.137	0.081	0.048
			40	0.114	0.056	0.033
		α_v	0	0.757	0.757	0.757
			20	0.722	0.514	0.342
			40	0.645	0.385	0.249
		ρ	0	0.672	0.672	0.672
			20	0.681	0.727	0.734
			40	0.700	0.748	0.766

TABLE 4 /CONTINUATION/

θ	$t^{\circ}\text{C}$	α_h, α_v ρ	$S\%$	λ cm		
				38	75	200
75	0	α_h	0	0.105	0.105	0.105
			20	0.105	0.089	0.059
			40	0.102	0.068	0.040
		α_v	0	0.826	0.825	0.825
			20	0.823	0.756	0.595
			40	0.810	0.648	0.458
		ρ	0	0.773	0.774	0.774
			20	0.774	0.790	0.819
			40	0.776	0.810	0.838
	20	α_h	0	0.110	0.110	0.110
			20	0.106	0.073	0.044
			40	0.096	0.052	0.030
		α_v	0	0.841	0.840	0.840
			20	0.826	0.682	0.489
			40	0.785	0.543	0.367
		ρ	0	0.768	0.769	0.769
			20	0.772	0.805	0.834
			40	0.782	0.827	0.847
	40	α_h	0	0.115	0.115	0.115
			20	0.105	0.062	0.036
			40	0.087	0.042	0.025
		α_v	0	0.855	0.855	0.855
			20	0.820	0.613	0.423
			40	0.746	0.473	0.315
		ρ	0	0.764	0.764	0.764
			20	0.772	0.816	0.841
			40	0.790	0.836	0.852

TABLE 4 /CONTINUATION/

ϕ	$T^{\circ}C$	$\alpha_p \alpha_v$	$S\%$	λ cm		
				18	75	200
80	0	α_h	0	0.072	0.072	0.072
			20	0.072	0.060	0.040
			40	0.070	0.046	0.027
		α_v	0	0.941	0.942	0.942
			20	0.937	0.883	0.737
			40	0.925	0.786	0.594
		ρ	0	0.858	0.858	0.858
			20	0.857	0.872	0.897
			40	0.860	0.889	0.912
	20	α_h	0	0.075	0.075	0.075
			20	0.073	0.050	0.030
			40	0.066	0.035	0.020
		α_v	0	0.952	0.952	0.952
			20	0.938	0.817	0.629
			40	0.903	0.684	0.491
		ρ	0	0.853	0.853	0.853
			20	0.856	0.884	0.909
			40	0.865	0.903	0.920
	40	α_h	0	0.078	0.078	0.078
			20	0.072	0.042	0.025
			40	0.059	0.029	0.017
		α_v	0	0.960	0.961	0.961
			20	0.932	0.752	0.556
			40	0.869	0.610	0.429
		ρ	0	0.849	0.849	0.849
			20	0.856	0.894	0.915
			40	0.872	0.910	0.924

TABLE 4 /CONCLUSION/

ϕ	$t^{\circ}\text{C}$	$\frac{\alpha_h}{\alpha_v}$	$S\%$	λ cm		
				18	75	200
85	0	α_h	0	0.037	0.037	0.037
			20	0.037	0.031	0.020
			40	0.036	0.023	0.014
		α_v	0	0.988	0.990	0.990
			20	0.981	0.965	0.901
			40	0.970	0.922	0.809
		ρ	0	0.928	0.928	0.928
			20	0.928	0.938	0.956
			40	0.929	0.951	0.966
	20	α_h	0	0.039	0.038	0.038
			20	0.037	0.026	0.015
			40	0.033	0.018	0.010
		α_v	0	0.985	0.985	0.985
			20	0.975	0.935	0.833
			40	0.958	0.866	0.721
		ρ	0	0.925	0.925	0.925
			20	0.927	0.947	0.964
			40	0.932	0.960	0.972
	40	α_h	0	0.040	0.040	0.040
			20	0.037	0.021	0.012
			40	0.030	0.014	0.005
		α_v	0	0.980	0.980	0.980
			20	0.965	0.902	0.778
			40	0.941	0.817	0.659
		ρ	0	0.921	0.921	0.921
			20	0.927	0.954	0.959
			40	0.938	0.965	0.974

1. Debye, P., and Zakk, G., Teoriya elektricheskikh svoystv molekul /Theory of the Electrical Properties of Molecules/, Moscow-Leningrad, ONTI, 1936.
2. Hipple, A. R., Dielektriki i volny /Dielectrics and Waves/, Moscow, IL, 1962.
3. Hasted, J. B., "The Dielectric Properties of Water," Progress in Dielectrics, London, 1961, 3.
4. Ray, P., Appl. Opt. 11(8), 1836-1844 (1972).
5. Krasnyuk, N. P., and Rozenberg, V. N., Korabel'naya radiolokatsiya i meteorologiya /Marine Radar and Meteorology/, Leningrad, "Sudostroyeniye", 1970.
6. Wu, S. T., and Funk, A. K., J. Geophys. Res. 77(30), 5917-5929 (1972).
7. Rabinovich, Yu. I., and Melent'yev, V. V., Trudy GGO /Transactions of Main Geophysical Observatory/, Leningrad, "Gidrometeoizdat", 1970, No. 235, pp. 78-123.
8. Gray, K., Hall, W., Hardy, W., Hide, G., Ho, W., Love, A., Van Melle, M., and Wang, H., Proc. 7th ISRSE, Ann Arbor, Michigan, 3, 1827-1845 (1971).
9. Akhadov, Ya. Yu., Dielektricheskiye svoystva chistyykh zhidkostey /Dielectrical Properties of Pure Liquids/, Moscow, "Standarty", 1972.
10. Kay, J., and Laby, T., Tablitsy fizicheskikh i khimicheskikh postoyannykh /Tables of Physical and Chemical Constants/, Moscow, "Fizmatgiz", 1962.
11. Stogryn, A., IEEE Tr. MTT 19(8), 733-736 (1971).
12. Peroslogin, S. V., Izv. AN SSSR. Fizika atmosfery i okeana 3(1), 45-57 (1967).
13. Lapley, L., and Adams, W., Water Resources Res. 7(6), 1538-1547 (1971).
14. Horn, R., Morskaya khimiya /Marine Chemistry/, Moscow, "Mir", 1972.

15. Korbanova, V. I., Fizicheskiye svoystva gornykh porod /Physical Properties of Rocks/, Moscow, "Gostoptekhnizdat", 1962.
16. Benoit, J. J., J. Phys. Radium 5, 255 (1944). /46
17. Conner, W. P., and Smyth, C. P., J. Amer. Chem. Soc. 65, 382 (1943).
18. Grant, E. H., Buchanan, T. J., and Cook, H. F., J. Chem. Phys. 26, 156 (1957).
19. Saxtion, J. A., and Lane, J. A., Report Phys. and Roy. Met. Soc., 278 (1947).
20. Moreno, T., Microwave Tr. Design Data, New York, 1948.
21. Lamb, J., Tr. Faraday Soc. 42A, 108 (1946).
22. Tamm, K., and Scheider, M., Z. angew. Phys. 20, 544 (1966).
23. Clevogt, K. E., Ann. Phys. 36, 141 (1939).
24. Rabinovich, Yu. I., and Melent'yev, V. V., Trudy GGO, Leningrad, "Gidrometeoizdat", 1970, No. 235, pp. 124-126.
25. Earth Resources Program, Synopsis of Activity, March, 1970, Manned Spacecraft Center, Houston, Texas, 1970.
26. Droppleman, J., Menella, R., and Evans, D., J. Geophys. Res. 75(30), 5909-5913 (1970).
27. Chen, S., and Peake, W., IRE Tr. AP-9(6), 567-572 (1961).
28. Yesepkina, N. A., Korol'kov, D. V., and Pariyskiy, Yu. N., Radioteleskopy i radiometry /Radiotelescopes and Radiometers/, Moscow, "Nauka", 1973.
29. Wilheit, T., Nordberg, W., Blinn, J., Campbell, W., and Edgerton, A., Remote Sens. Env. 2(3), 129-139 (1971/1972/). /file-
30. Shanda, E. J., Industries Atomiques and Spatioles 4, 65-80' (1972).
31. Thompson, E. J., Silberberg, R. W., Gray, K. W., and Hardy, W. W., IEEE Tr. MTT 16(11), 938-943 (1968).
32. Lepley, L., and Adams, W., IEEE Tr. Geosci. Electr. 10(3), 140-155 (1972).

Real Part of Complex Dielectric Permittivity
of Sea and Fresh Water

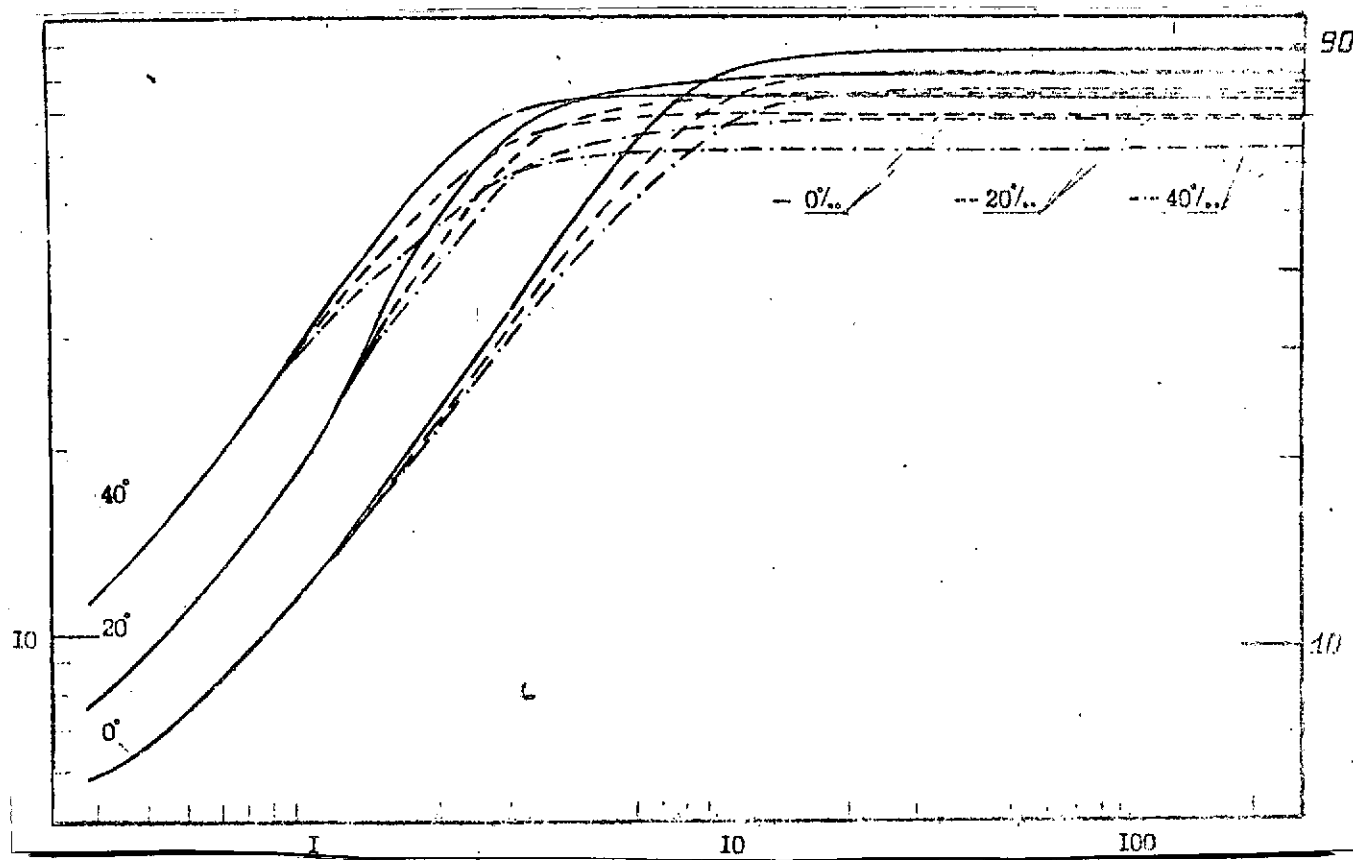


Fig. 1

Wavelength (cm)

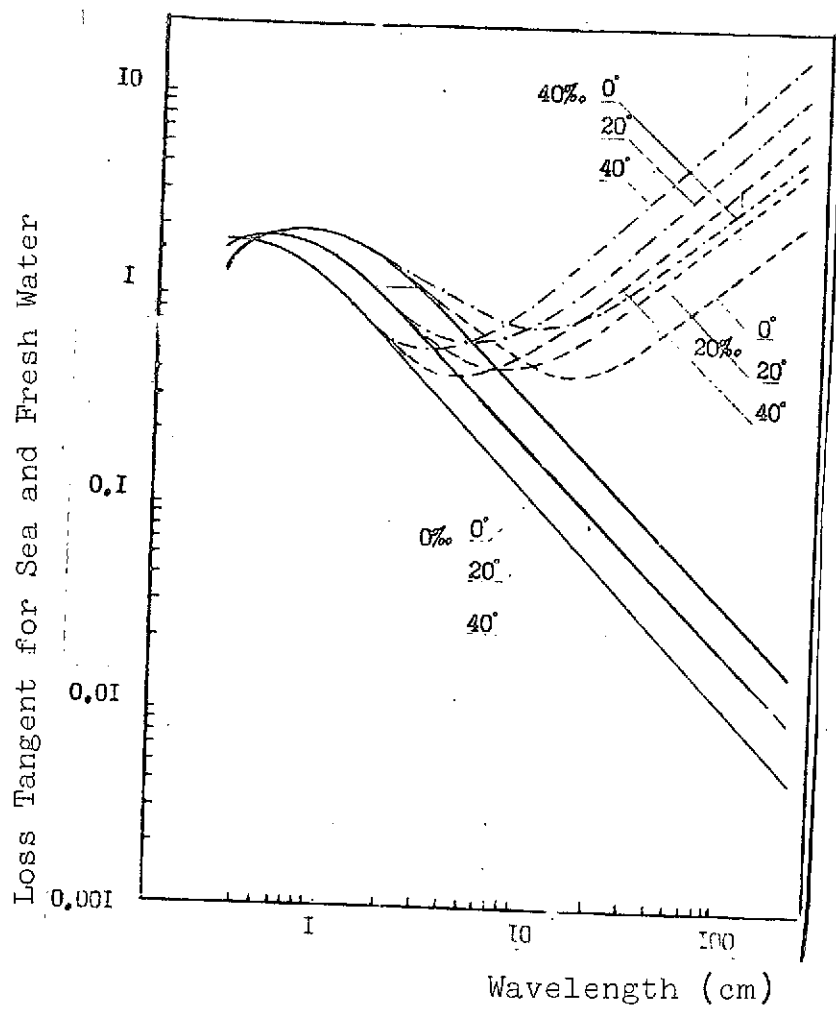


Fig. 2

Real Part of Dielectric Permittivity of Fresh Water

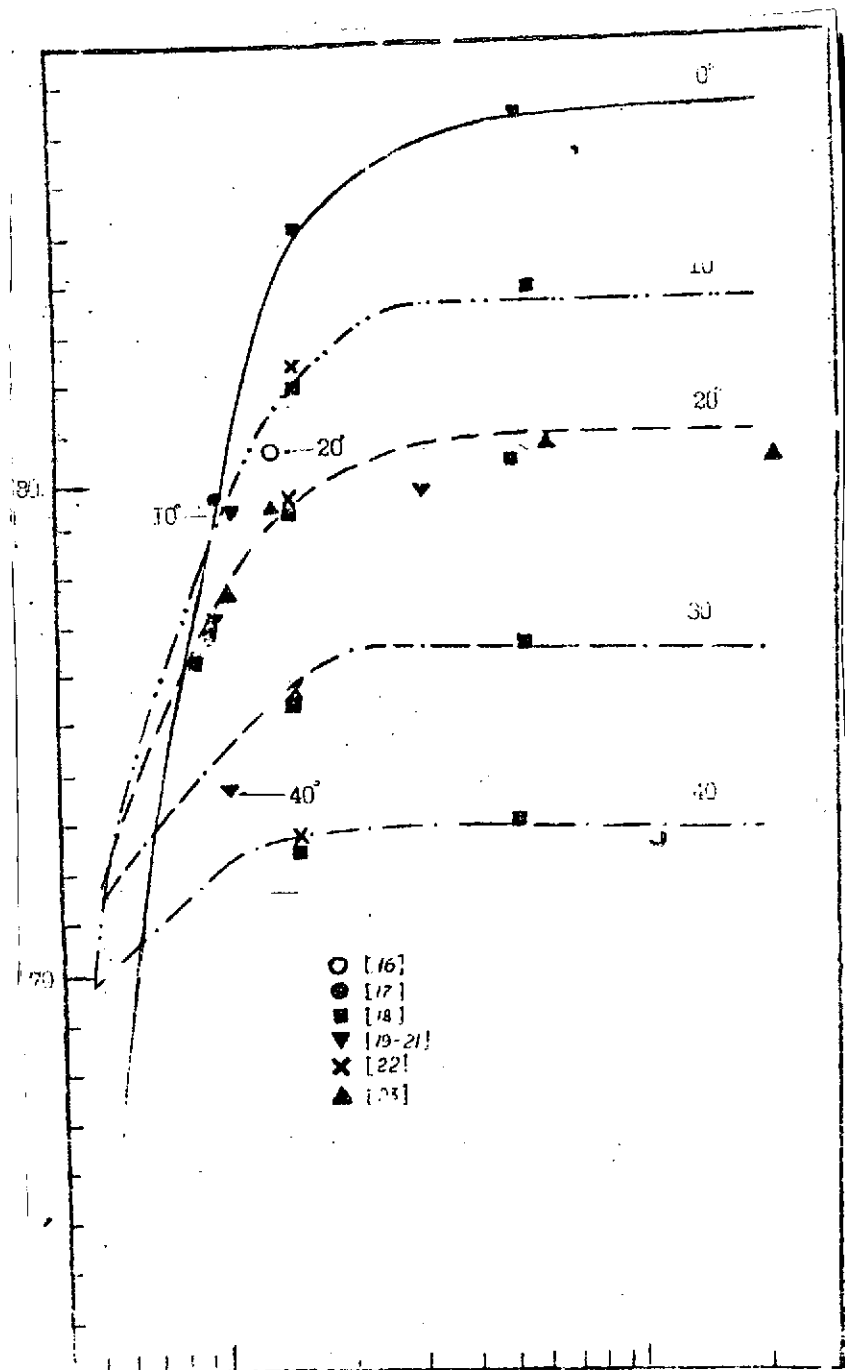


Fig. 3

λ (cm)

Loss Tangent for Fresh Water

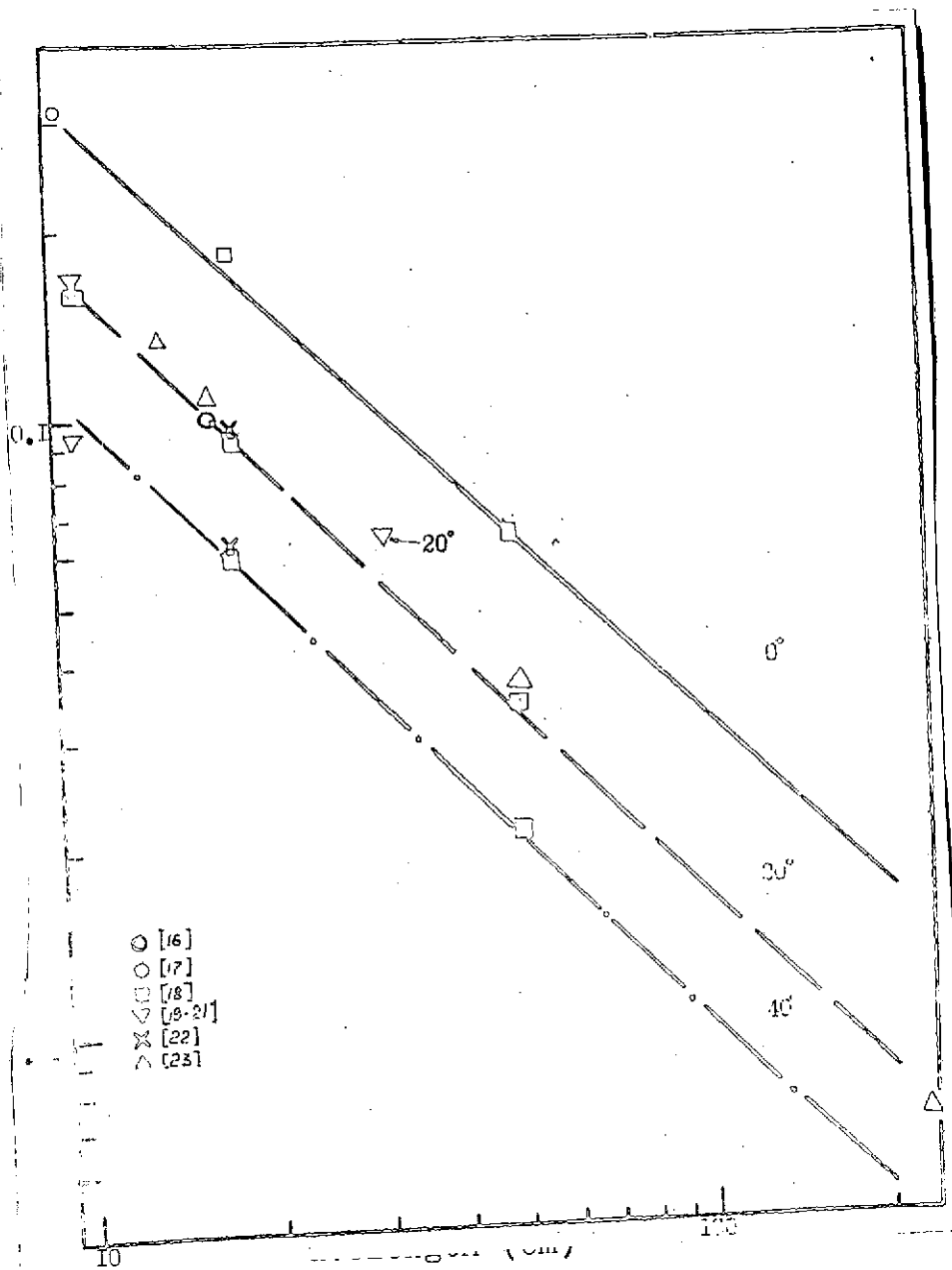
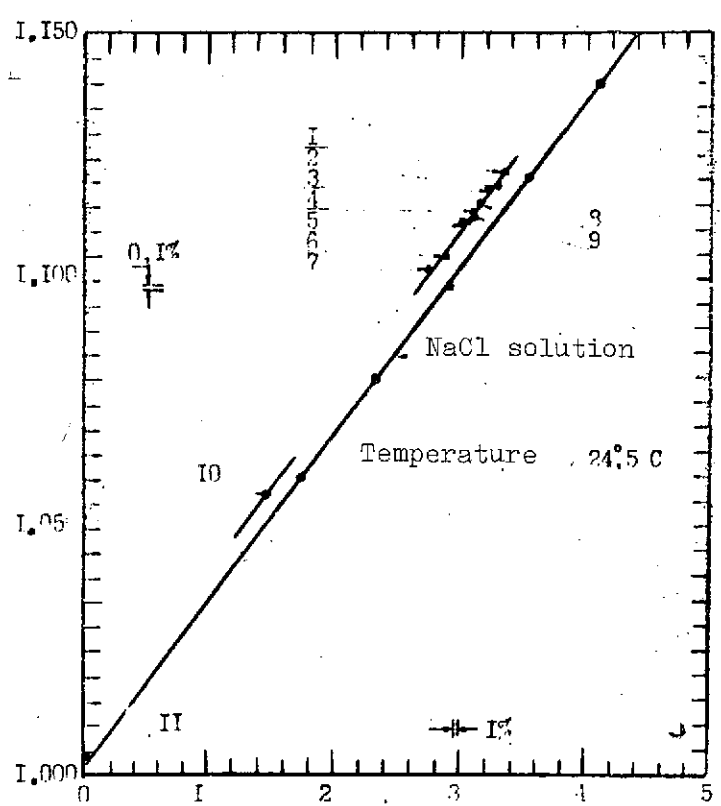


Fig. 4

Dielectric Constant ϵ' of NaCl Solution and
Fresh Water, $\epsilon'_{\text{fresh}} - 1$
 $\epsilon'_{\text{sea}} - 1$



Concentration (Weight percent)

1-10. Samples taken from different regions
of the World Ocean

1. 37°57' N: 68°27' W II. Tap water

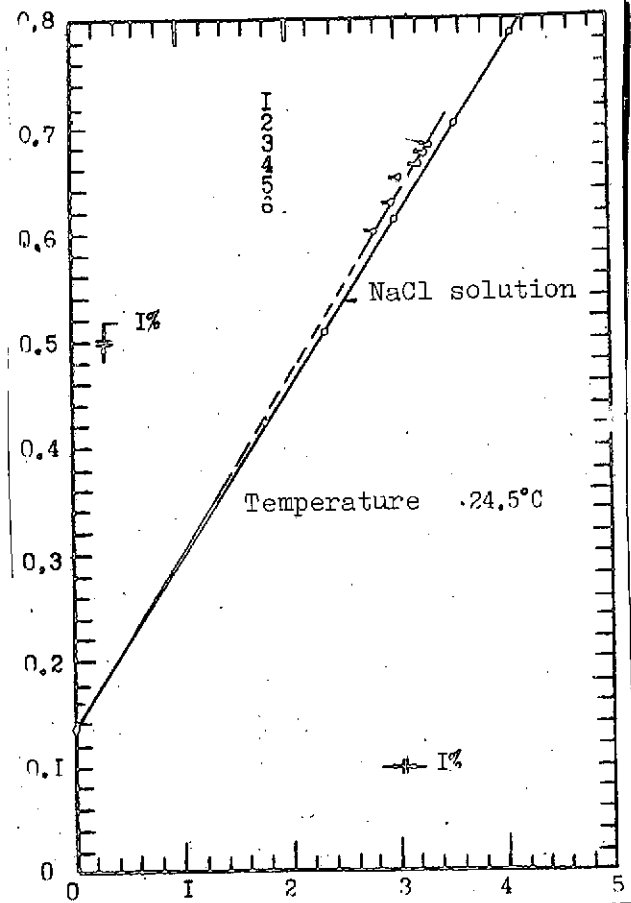
2. Hawaiian Islands

3. La Manche

8. 42° N: 155° E

Fig. 5

Dielectric Losses ϵ'' of NaCl Solution and
Sea Water $\frac{\epsilon''}{\epsilon' - 1}$



Concentration (Weight percent)

- 1-6. Samples taken from different regions
of the World Ocean
1. 37°57' N: 68°27' W
 2. Hawaiian Islands
 3. 42° N: 155° E

Fig. 6

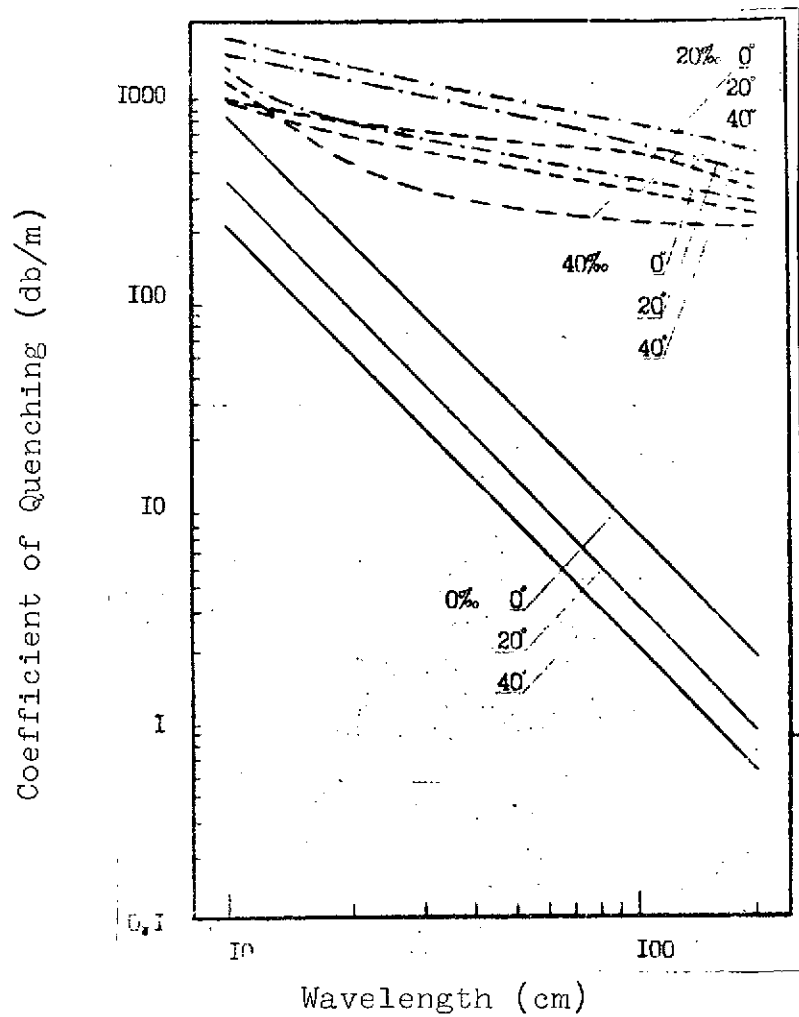


Fig. 7

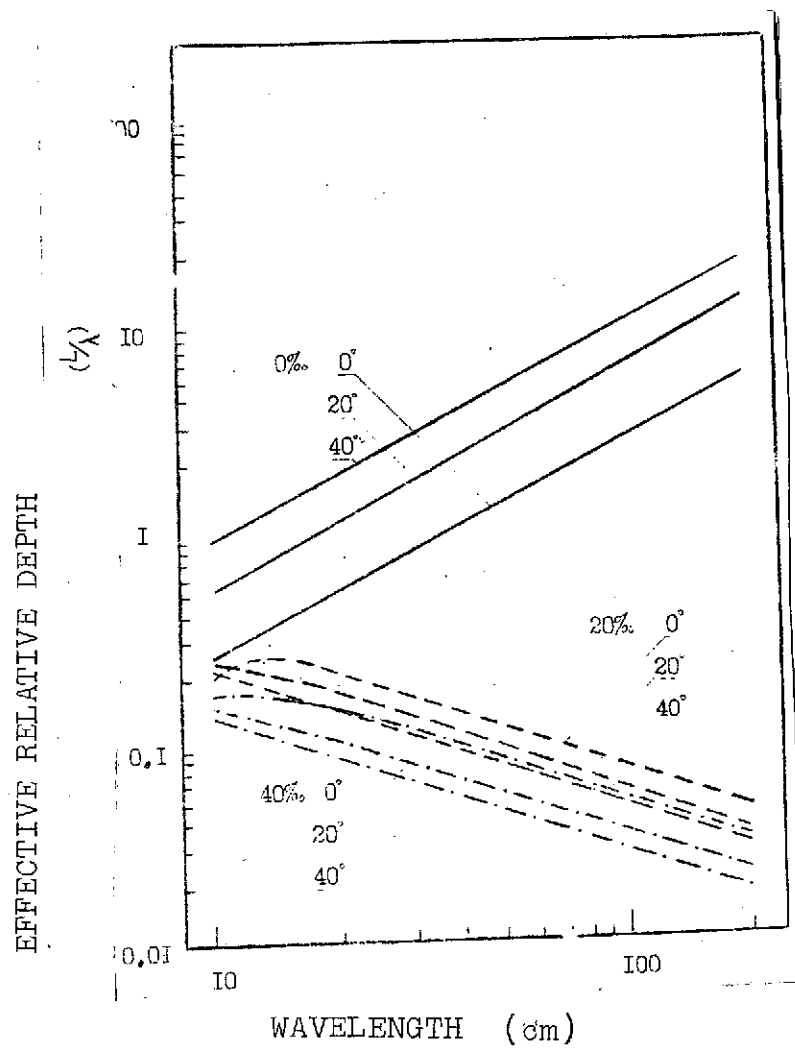
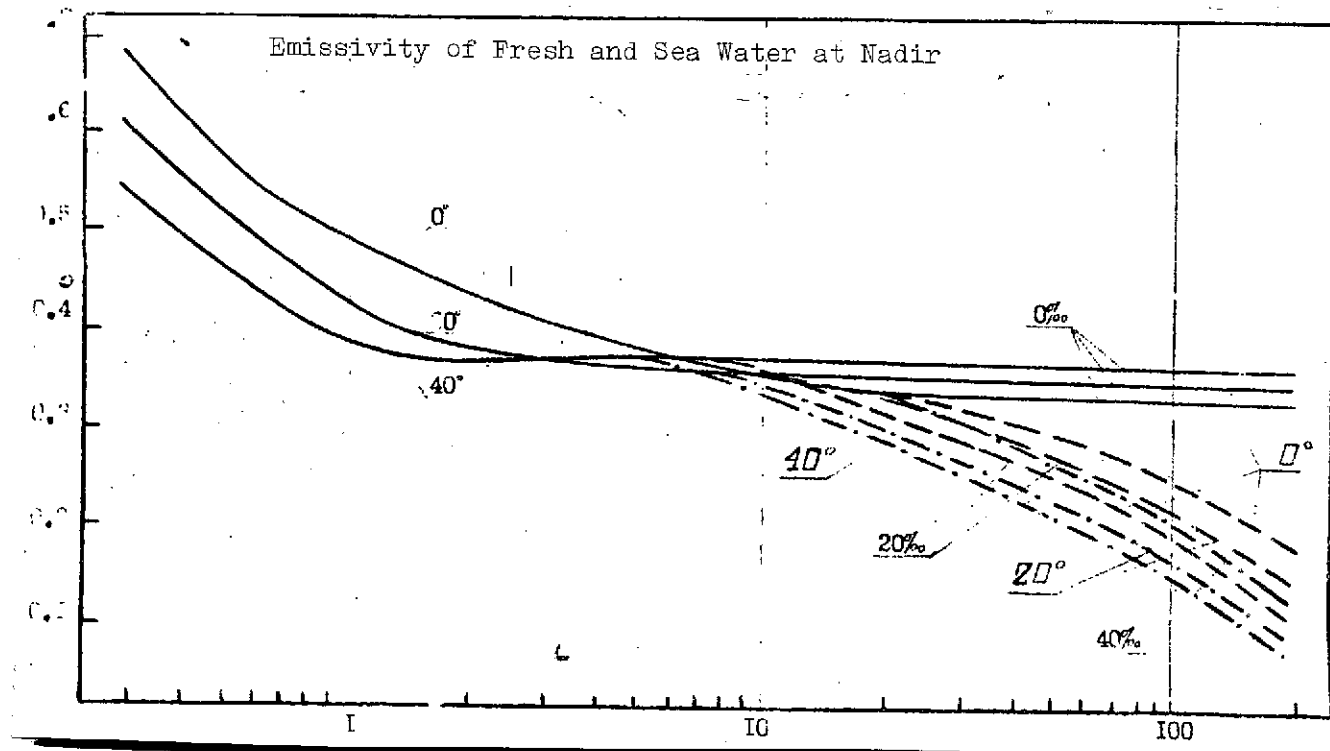


Fig. 8



Wavelength (cm)

Fig. 9

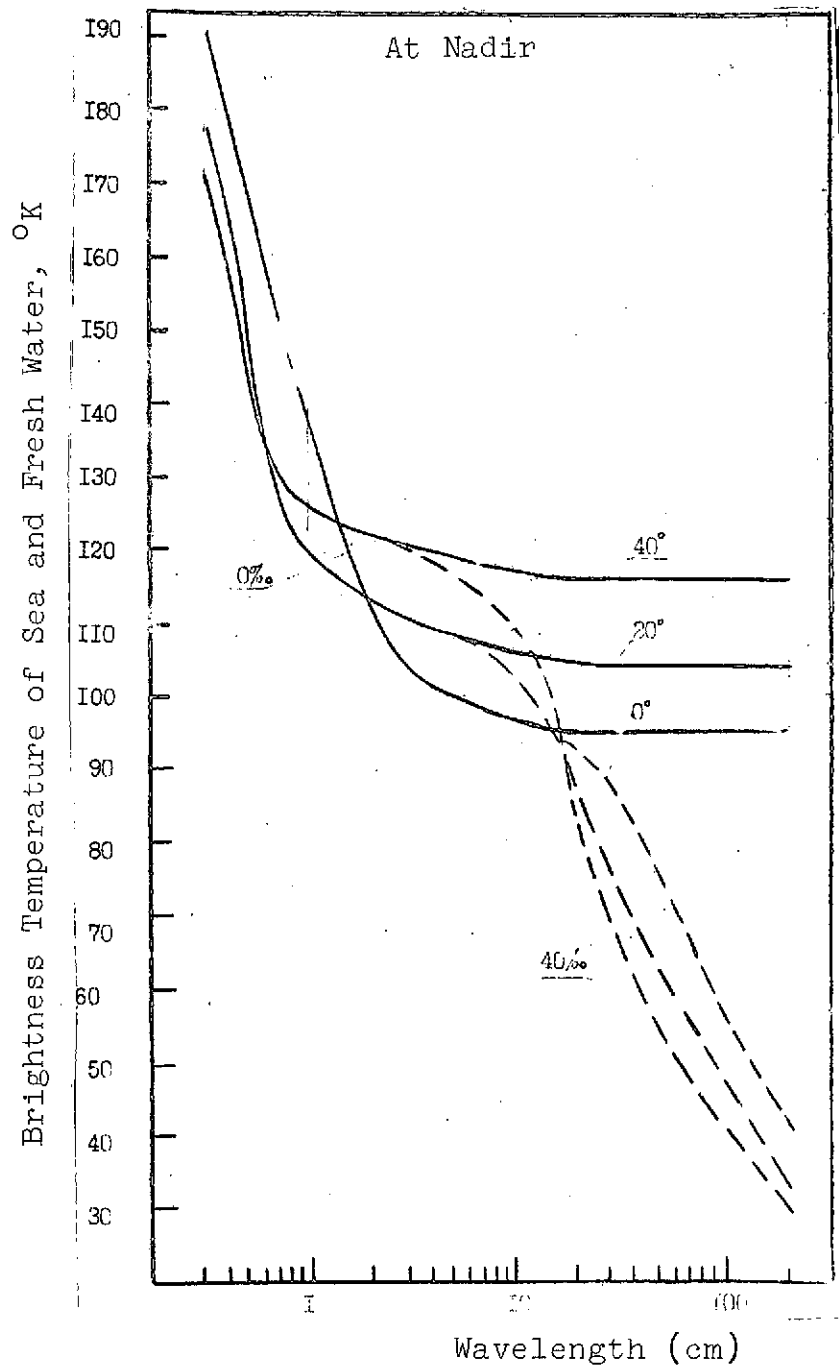


Fig. 10

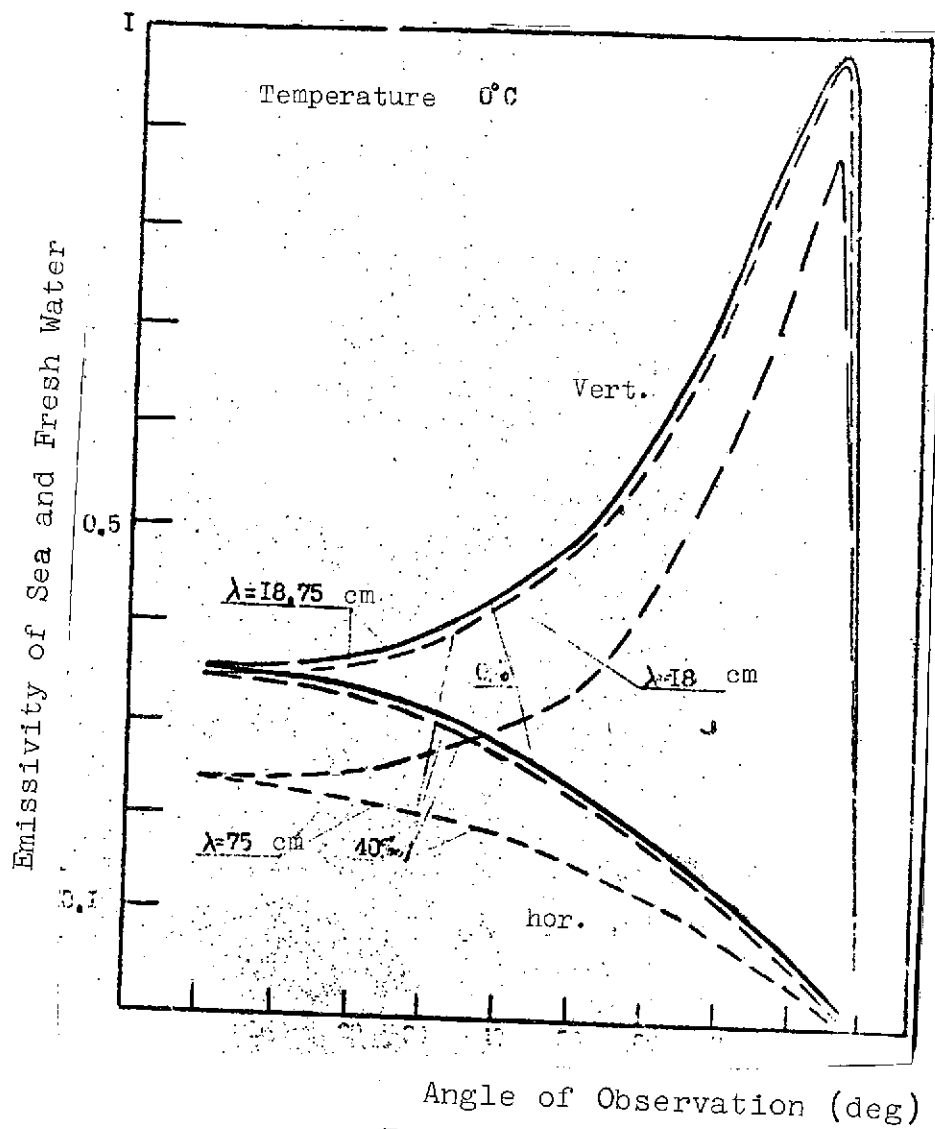


Fig. 11

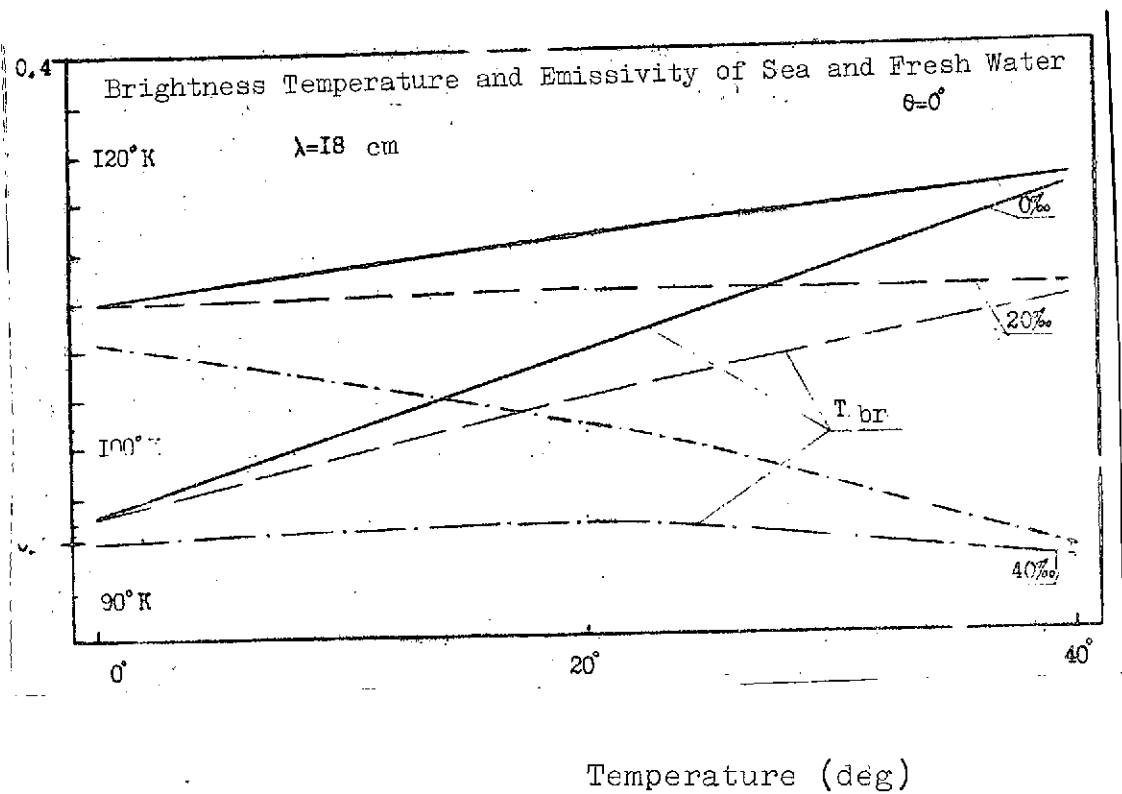


Fig. 12

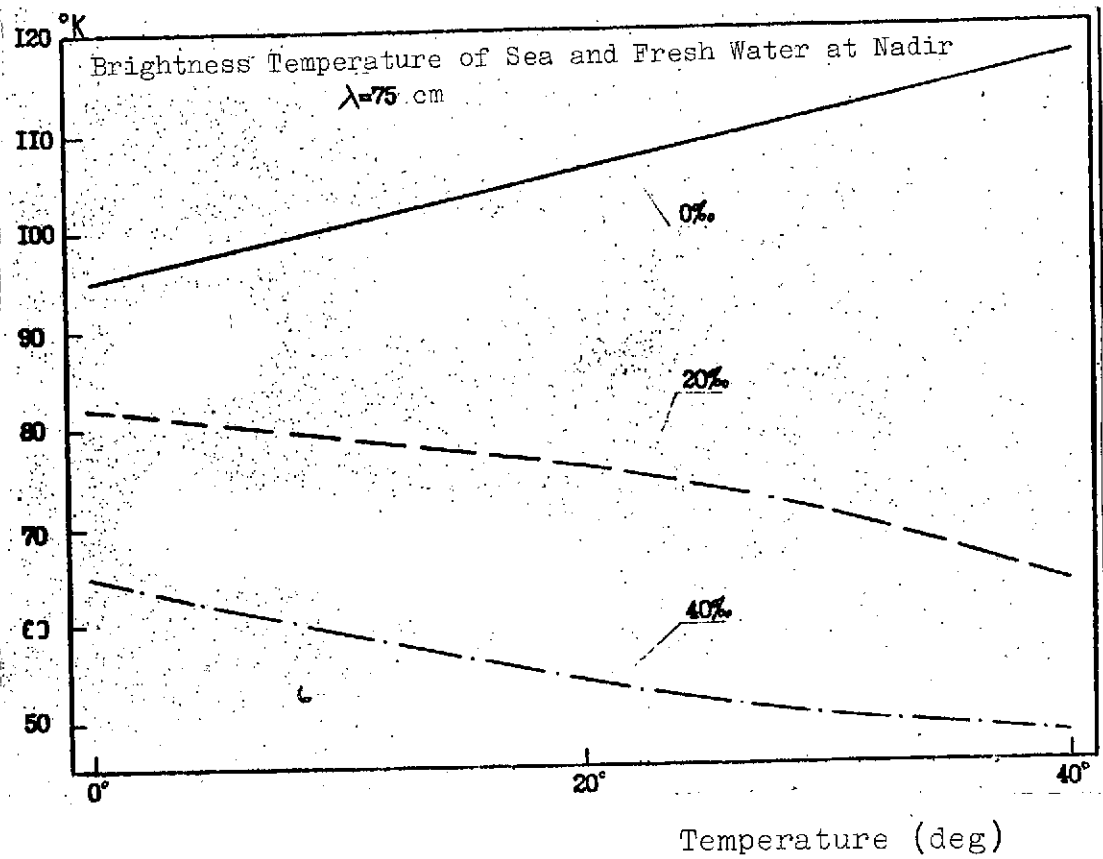


Fig. 13

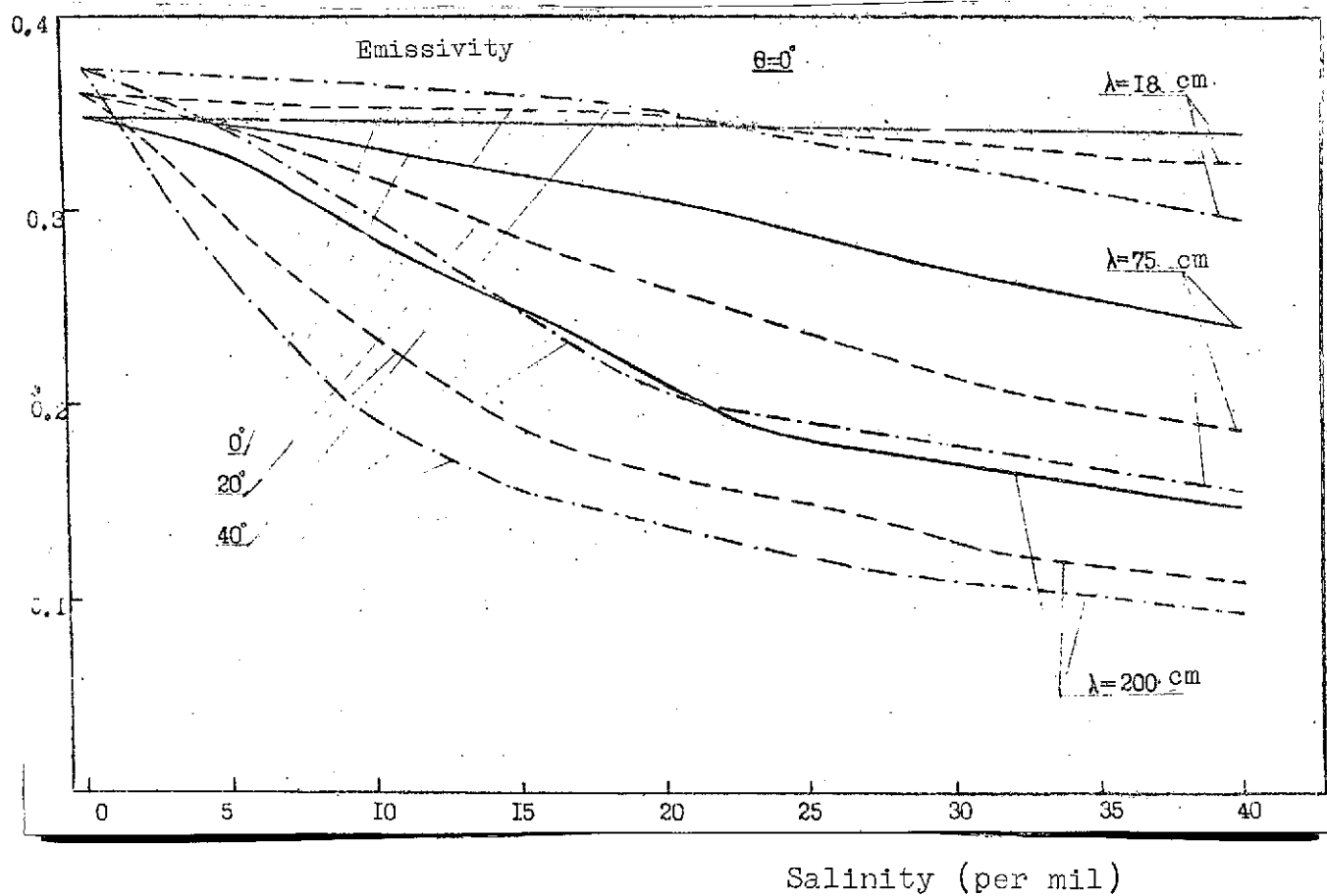


Fig. 14

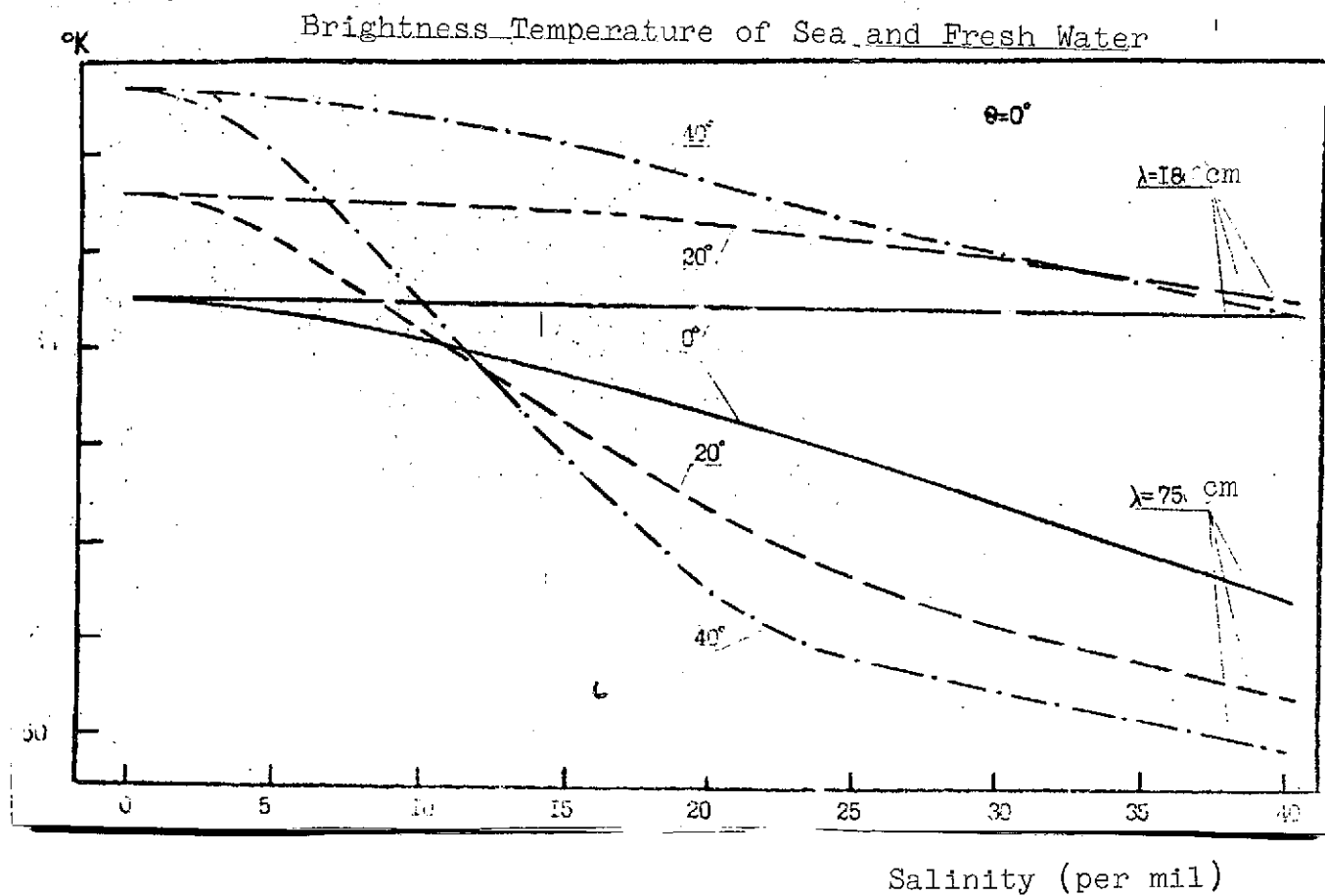
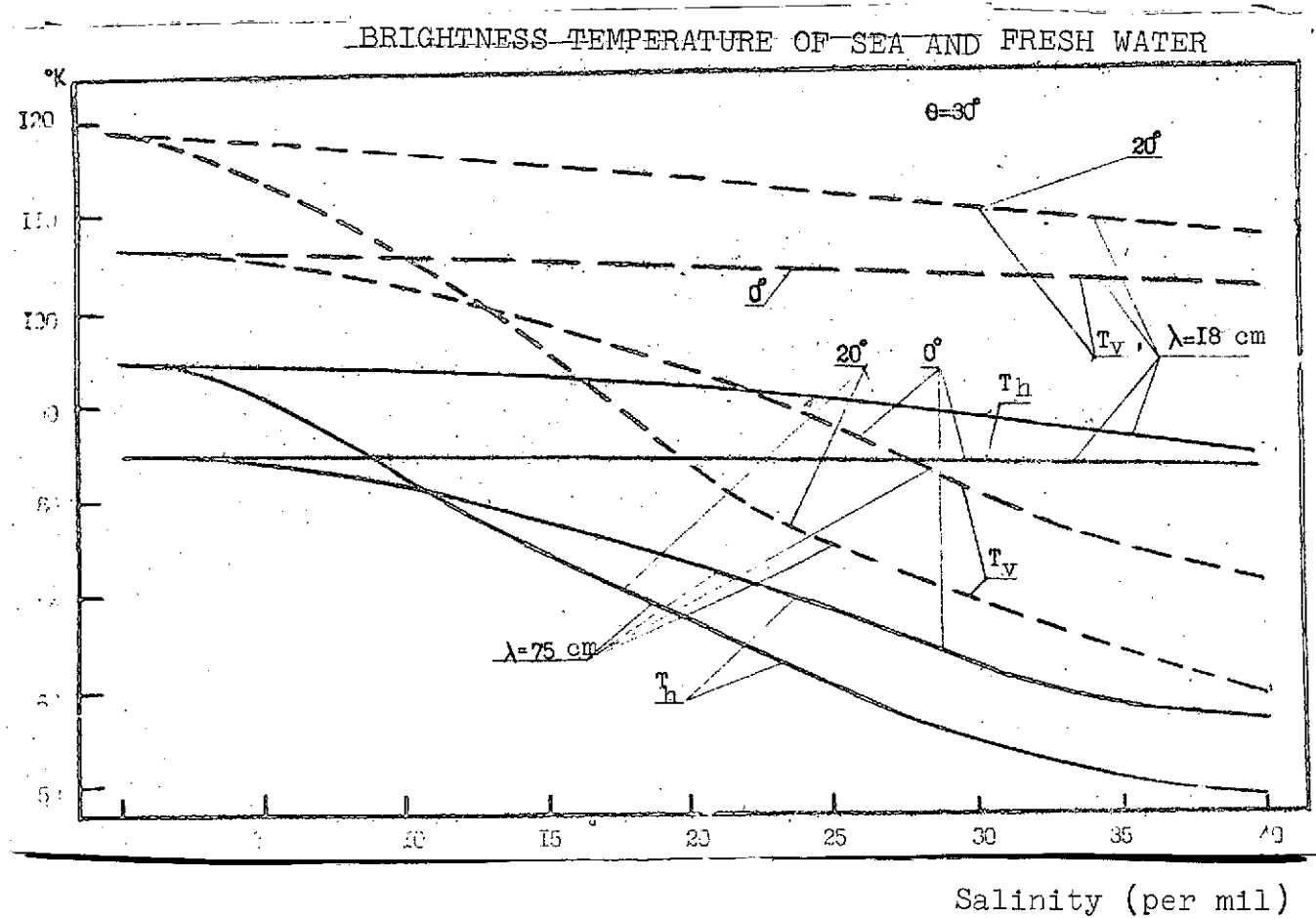
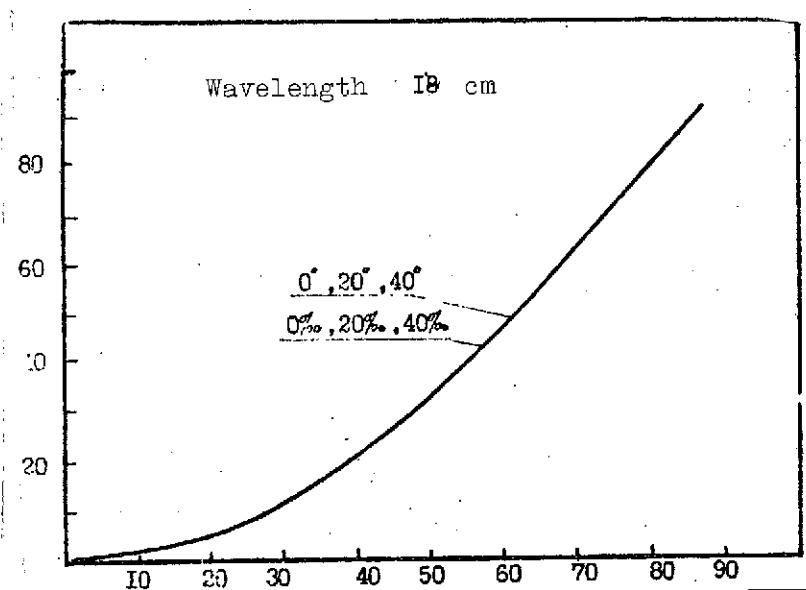


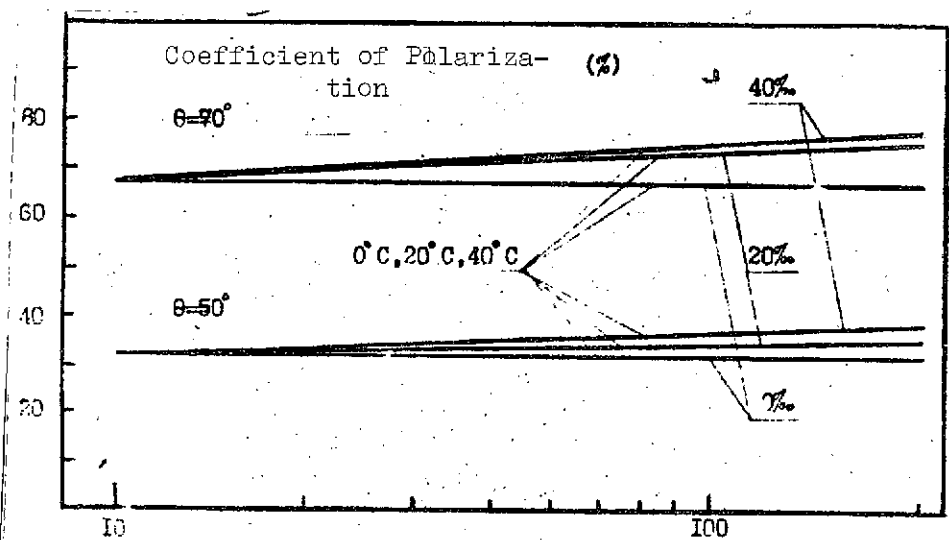
Fig. 15



Coefficient of Polarization (%)



Angle of Observation (deg)
Fig. 16



Wavelength (cm)
Fig. 17

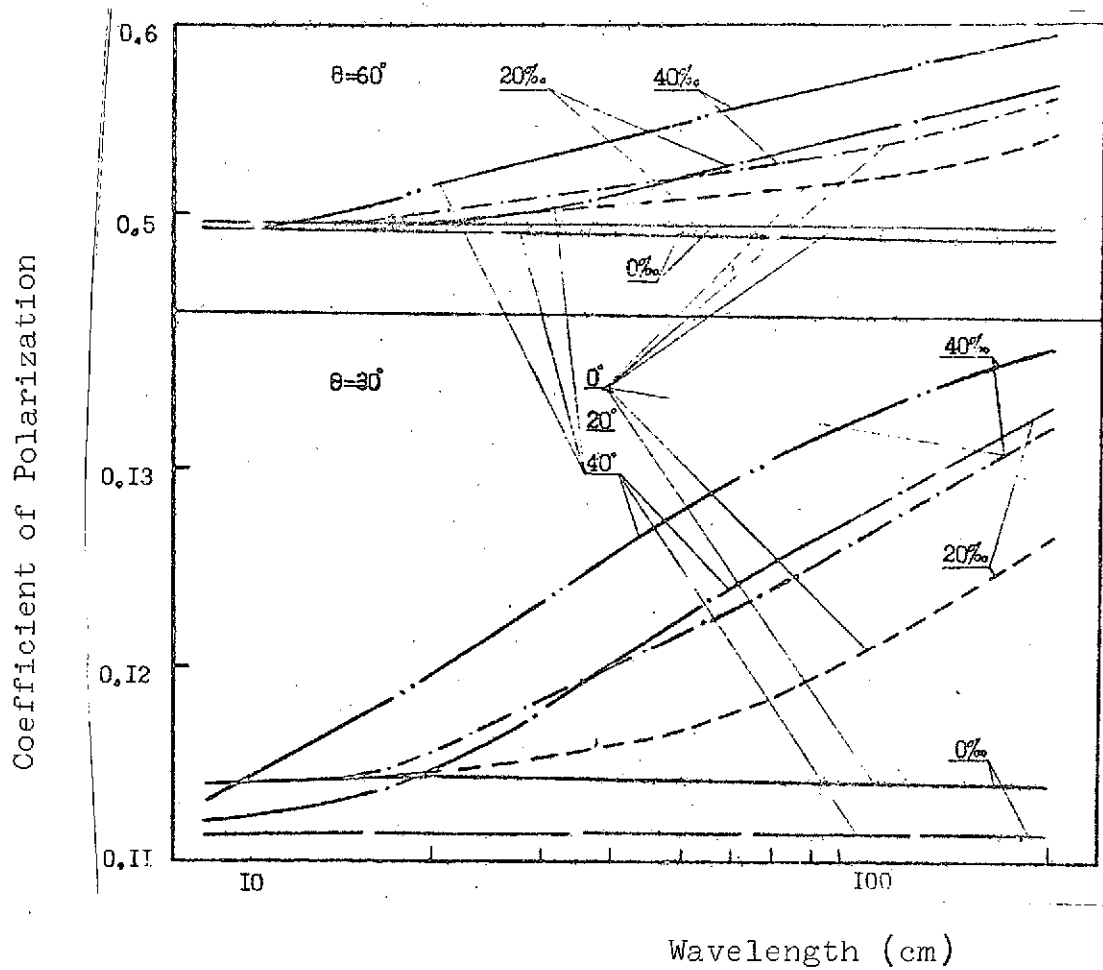


Fig. 18

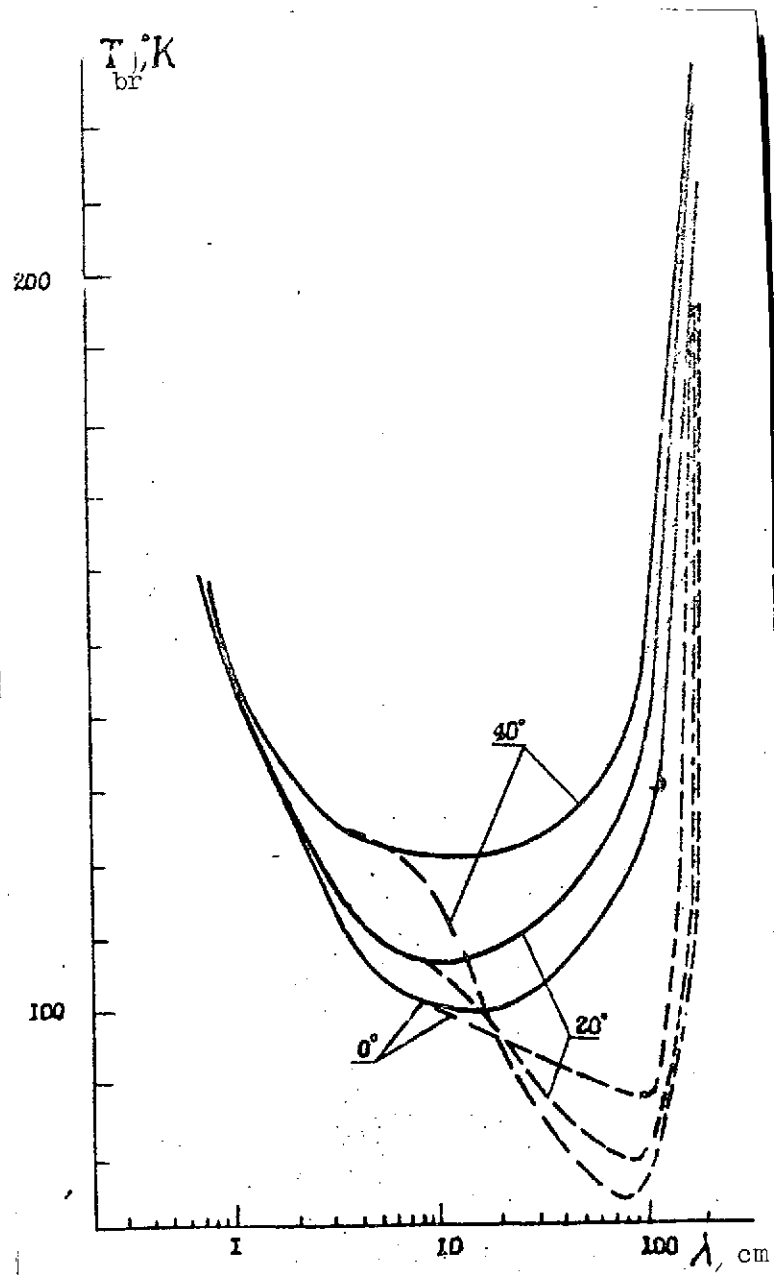


Fig. 19

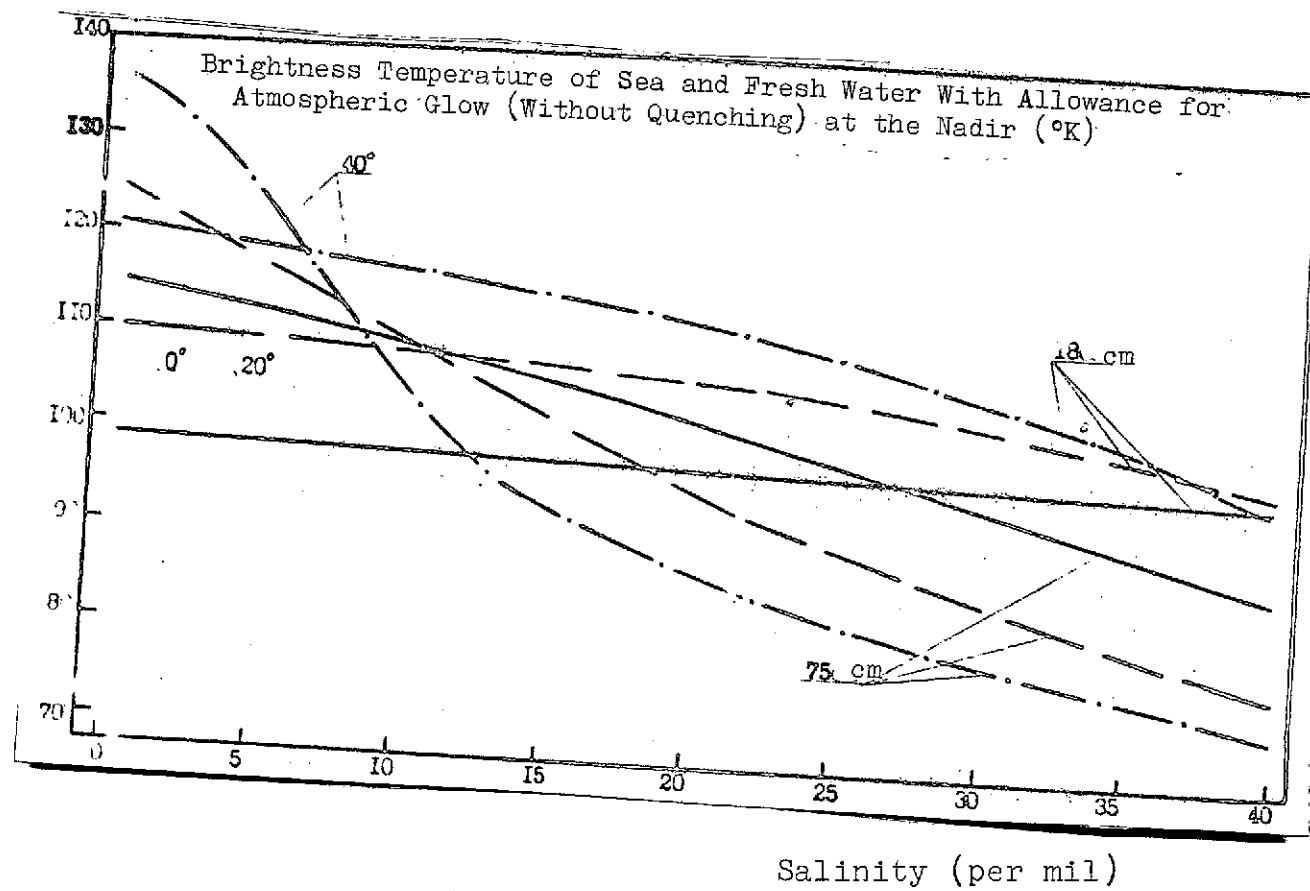


Fig. 20

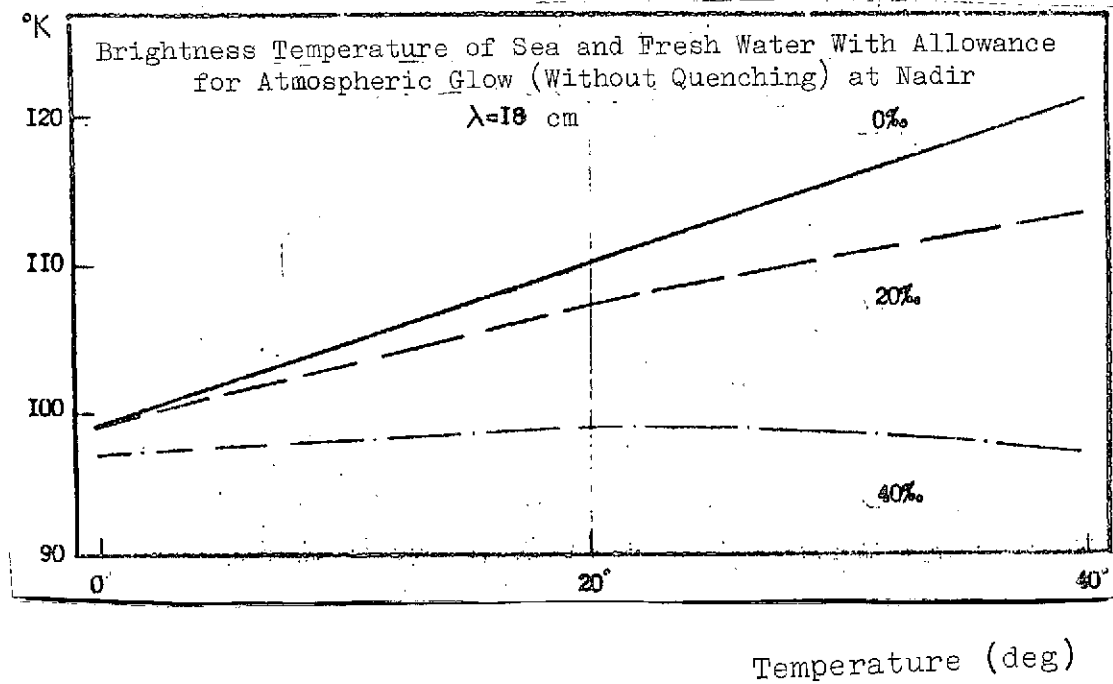


Fig. 21

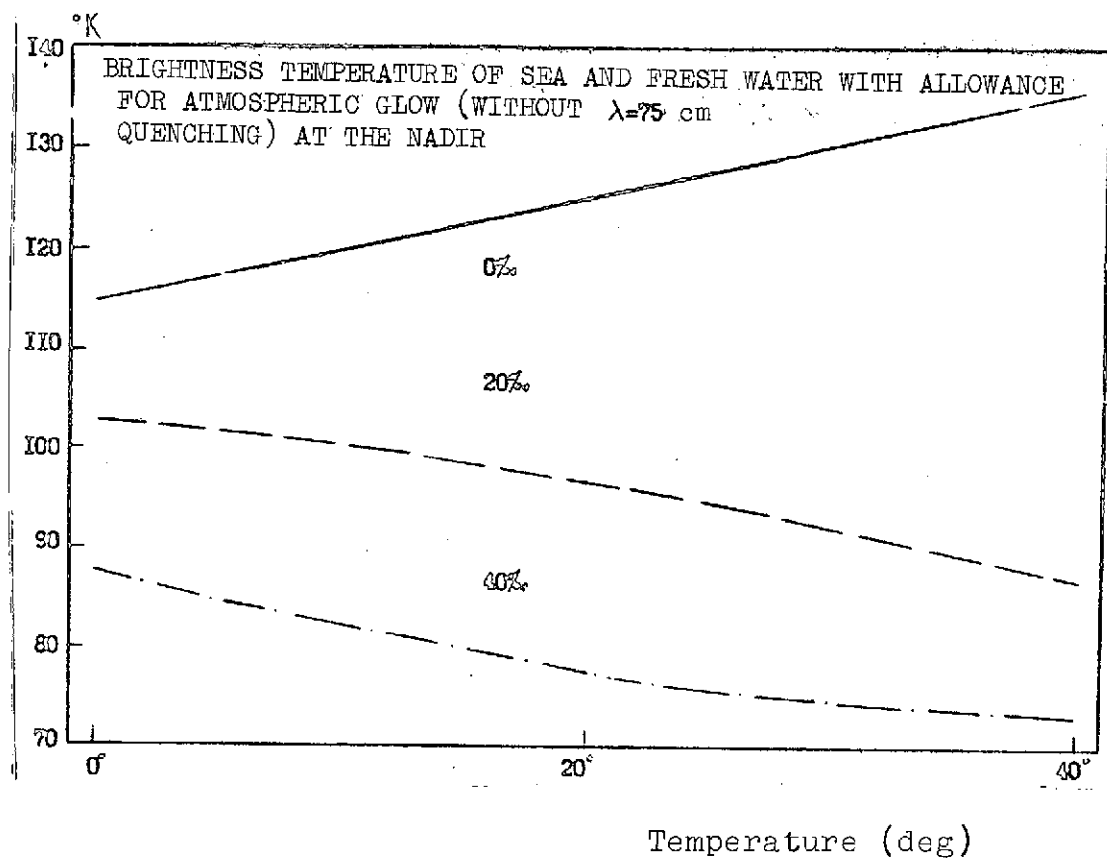


Fig. 22

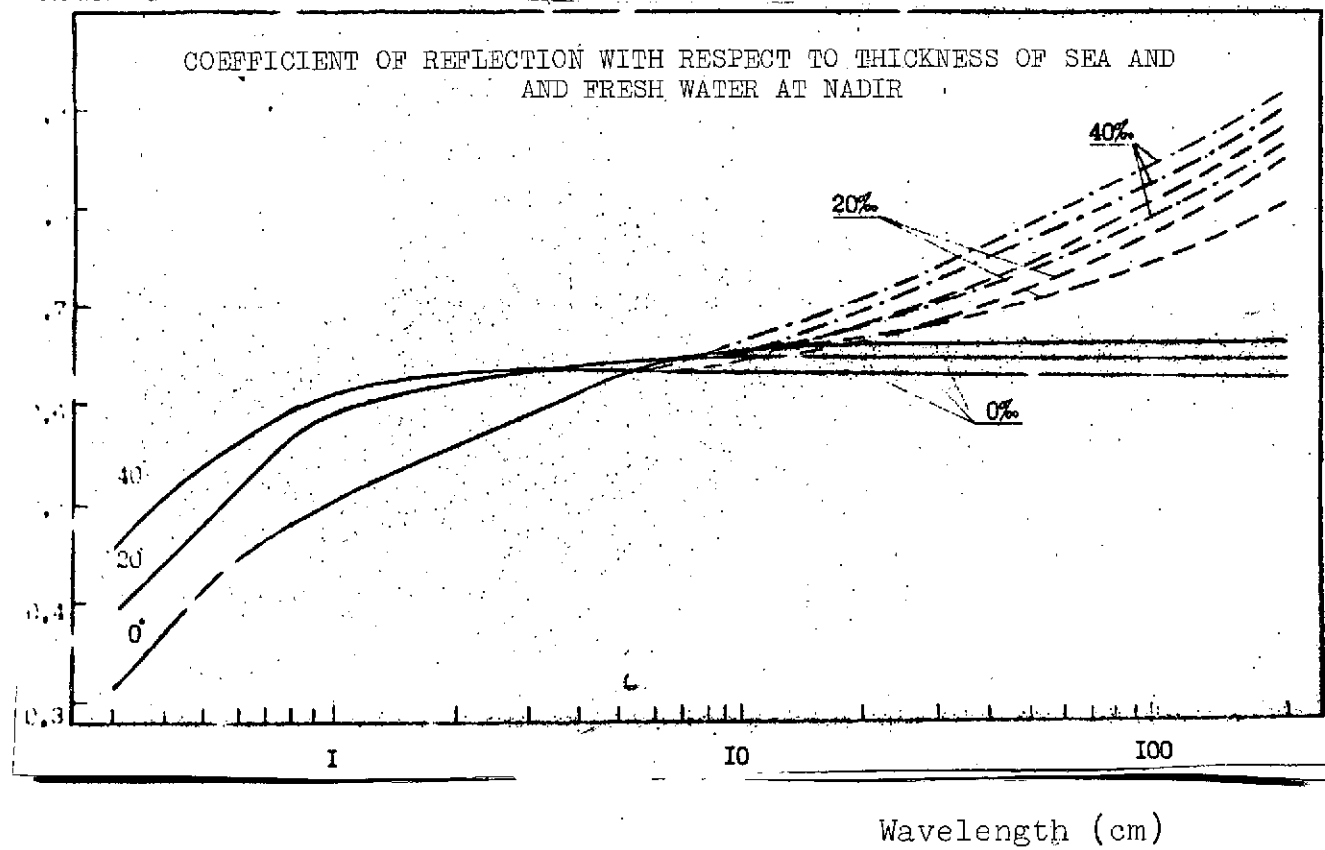


Fig. 23

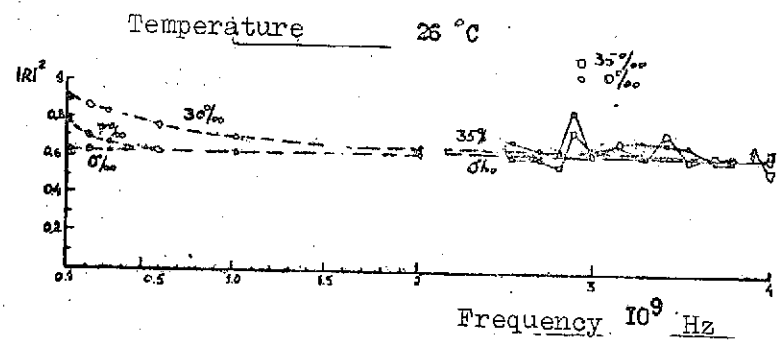
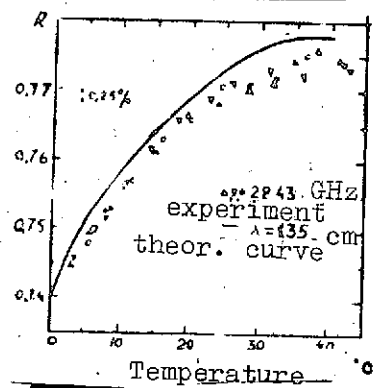
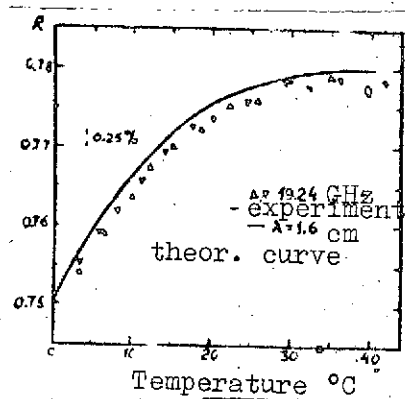


Fig. 24